AFOSR/DRA-62-13

AFOSR/DRA-62-13

AIR FORCE OFFICE OF SCIENTIFIC RESEARCH

TECHNICAL REPORT

ON THE NONLINEAR YAW MOTION OF A ROCKET SLED

Gerhard W. Braun

Harald A. Melkus

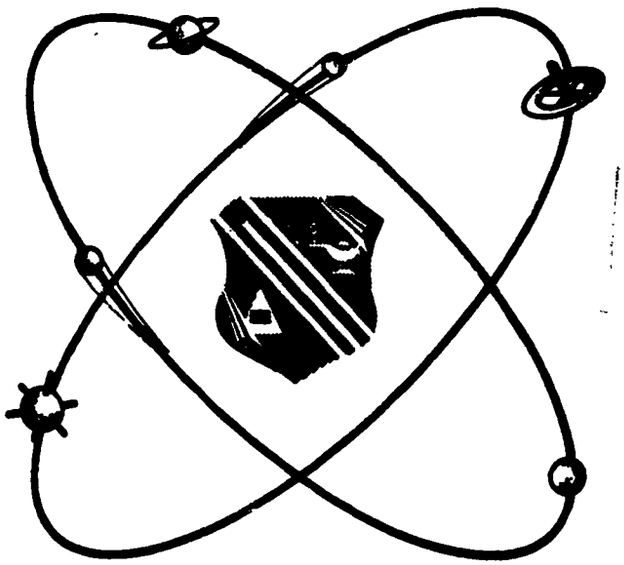

DIRECTORATE OF RESEARCH ANALYSES

HOLLOMAN AIR FORCE BASE

NEW MEXICO

July 1962

AFOSR/DRA-62-13

ON THE NONLINEAR YAW MOTION OF A ROCKET SLED

by

Gerhard W. Braun

Harald A. Melkus

Science and Engineering Analyses Division
Directorate of Research Analyses

AIR FORCE OFFICE OF SCIENTIFIC RESEARCH
OFFICE OF AEROSPACE RESEARCH
UNITED STATES AIR FORCE
Holloman Air Force Base, New Mexico

July 1962

FOREWORD

This study represents the joint effort of Dr. Gerhard W. Braun, Chief Scientist, Deputy for Development and Test, Air Force Missile Development Center, and Dr. Harald A. Melkus, Senior Aerospace Engineer, Fluid and Flight Mechanics, of the Directorate of Research Analyses, Air Force Office of Scientific Research, both at Holloman Air Force Base, New Mexico. The analysis was conducted in support of Project 6876, Track Facility Development, assigned to the Directorate of Guidance Test Facilities.

The results of the analysis were presented at the UNESCO Symposium on Nonlinear Oscillations, held in Kiev, USSR, in September 1961.

Sensitive guidance components and subsystems are affected by vibrations of the rocket sleds used in captive flight testing. A quantitative analysis of the vibrations induced during the motion of a sled along the rail is a prerequisite for finding means of reducing undesirable vibrations of rocket sleds. Answers must be obtained regarding the influence of damping, slipper play and aerodynamic stabilization on the dynamic behavior of the sled.

ABSTRACT

Some results are presented of an analog computer study concerned with the motion of a rocket sled configuration within a prescribed velocity profile. The motion of the sled was sidewise restricted by slippers running on rails.

The dynamic properties of the sled were studied under idealized conditions; it was assumed that the moving body has only two degrees of freedom; namely, lateral displacement and yaw. The body's weathercock stability was varied from negative to positive values as it was assumed that this aerodynamic property influences the mode of motion. The effects of damping and that of play between slipper and rail were studied to obtain indications as to how these parameters affect the motion.

This report is approved for publication.

James H. Ritter

JAMES H. RITTER
Colonel, USAF
Director, Research Analyses Directorate

TABLE OF CONTENTS

LIST OF ILLUSTRATIONS

NOMENCLATURE

x, y	coordinates of the c.g. of the sled
ψ	heading angle of sled
t	time, seconds
D	rail gage $D = 7$ ft (2.134 m)
T	thrust, if positive, or braking force, if negative, lb
$S_1 \cdots S_4$	cross forces on the slippers, positive in direction of positive y-axis, lb
$U = U(t)$	magnitude of velocity of the center of gravity of the sled in x-direction, ft sec^{-1}
ρ	density of air, lb ft^{-4} sec^2
$Y = c_y \frac{\rho}{2} U^2 D^2$	aerodynamic cross force, lb
I_z	moment of inertia of the sled around the vertical axis through the center of gravity, lb ft sec^2
K	spring constant, lb ft^{-1}
β	angle of yaw of the sled ($\beta = \psi - \frac{\dot{y}}{U}$)
ϵ	displacement of slippermark in direction of positive y, ft
ϵ_i, ϵ_o	inner and outer play of slippers, ft

Subscripts

Subscript 1 refers to left front slipper

Subscript 2 refers to right front slipper

Subscript 3 refers to left rear slipper

Subscript 4 refers to right rear slipper

Subscript F refers to front beam

Subscript R refers to rear beam

ON THE NONLINEAR YAW MOTION OF A ROCKET SLED

I. INTRODUCTION

In missilry, environmental tests have become of ever-increasing importance. It is well known that systematic errors are generated in high precision instruments—such as guidance systems—when subjected to the shock and vibration environment of a missile. Their compensation requires a calibration under closely simulated conditions or, in other words, a proper reproduction of the missile environment.

In search for means to simulate the missile environment the similarity between a supersonic sled and a missile has been early recognized. As a matter of fact one may call a rocket sled a rail guided missile. Figure 1 and Figure 2 are typical examples of rocket sleds and illustrate this similarity.

There are, however, important differences between missiles and sleds which cause also differences in their internal environments. The most conspicuous differences are perhaps the presence of the slipper beams and slippers as well as the absence of tailplanes for the sled. Therefore, one can expect that the main difference in the environment of the two vehicles is introduced by forces generated in these two elements.

For a quantitative appraisal of effects caused by these forces, the problem was simplified in the following manner: first, it was assumed that the sled moves on straight rails, and, second, its motion is limited to two degrees of freedom—that of a sideward translation and that of a rotation about a vertical axis. The case of straight rails is of practical interest as it represents the ideal condition one might closely approach by a most careful aligning,

grinding and smoothing the rails as has been done for quite some time on the Holloman track. At the same time, it appears that the confinement to straight rails does not represent a serious handicap; it will be seen that certain typical characteristics of the motion would occur even if the rails were perfectly straight. With regard to the other simplification the circumstances are similar. Here again it can be expected that the typical properties of the motion--important for the detection of parameters affecting the stability of a sled--will be preserved to a great extent.

In search for means to improve the stability the aerodynamic properties of the moving sled were incorporated in the analysis. As a rule a sled without a tailplane has no weathercock stability; in order to keep a sled on a straight path, rather high and frequent lateral slipper forces are required. On the other hand, by equipping a sled with fins one might expect that the generated aerodynamic force will contribute to the stabilization of its motion. The behavior of a sled should become similar to that of an aerodynamically stabilized missile in free flight provided: (1) the sled is equipped with sufficiently large fins, and (2) the play between slippers and rails is made so large that lateral disturbances are not strong enough to cause the slippers to touch the rails from the side.

For the reasons stated above the idealized case of a sled with different degrees of weathercock stability moving on straight rails and confined to small translations in lateral direction as well as to small yaw angles became the subject of an investigation.

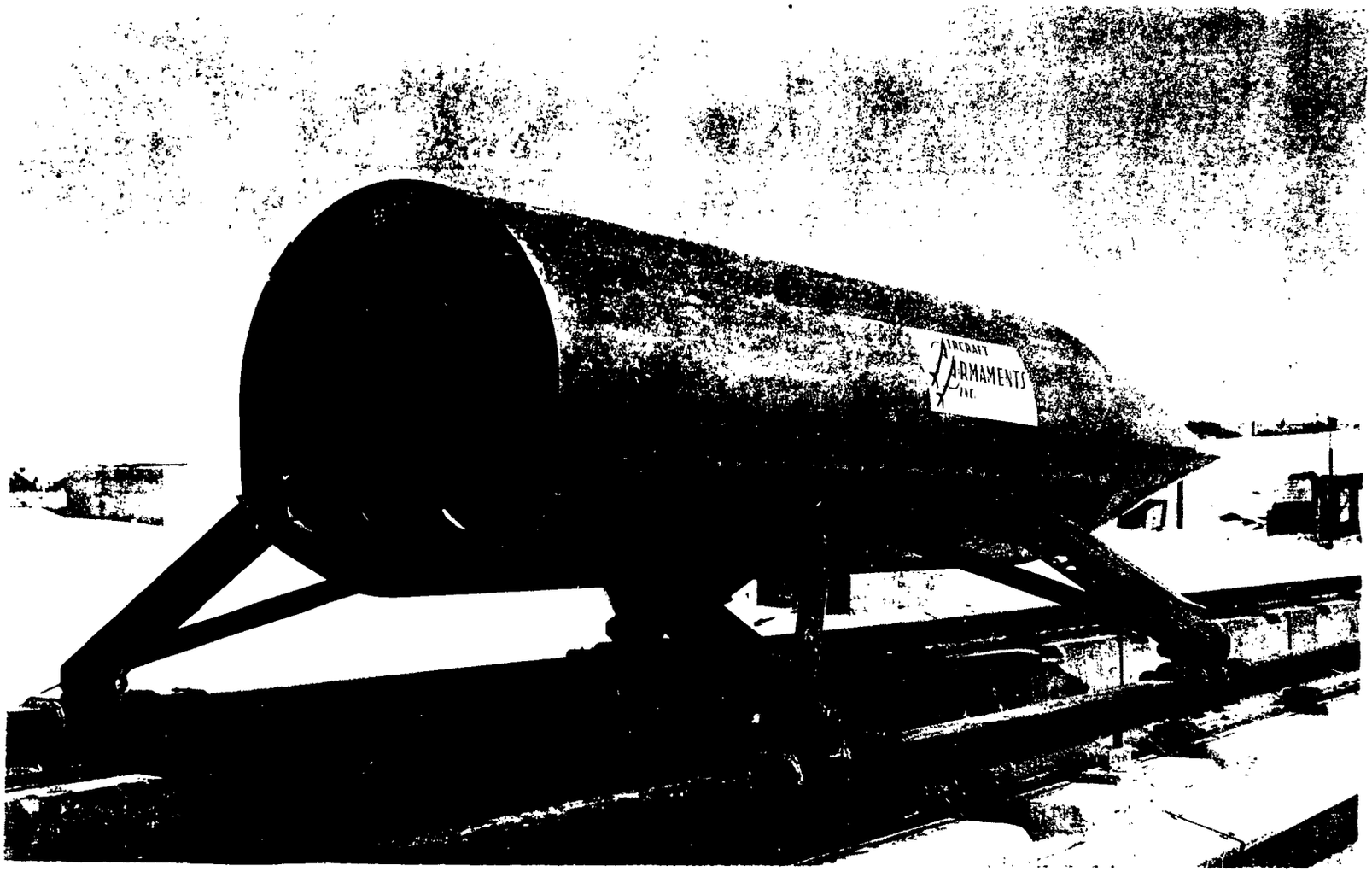

FIGURE 1. DUAL RAIL SLED

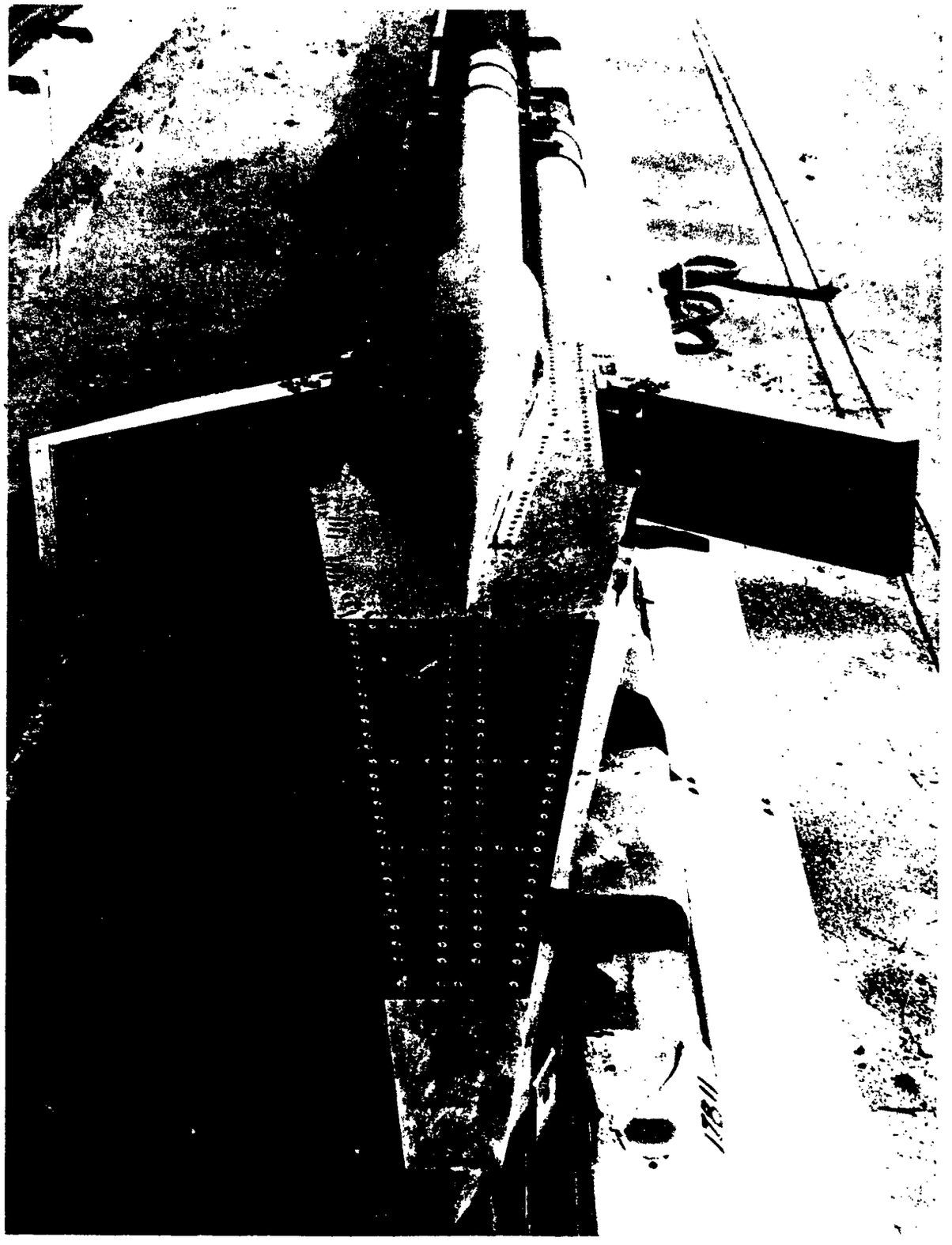

FIGURE 2. MONORAIL SLED

II. DESCRIPTION OF THE SLED AND RAILS

For the environmental tests mentioned before a sled configuration consisting of a pusher and forebody is mostly used. Figure 3 is a photograph of such a sled configuration. The test specimen is mounted in the forebody and the only connection between forebody and pusher is the coupling point. The coupling has the form of a universal joint which also provides a lateral degree of freedom (Fig. 4). Due to the ever-present vibrations, friction forces in lateral direction can be expected to be small. In the following investigation they are completely neglected. This is to say that the thrust force, transmitted from the pusher to the forebody is assumed to be always aligned in a direction parallel to the rails.

On a sled, vibrations are produced by thrust irregularities and by aerodynamic effects such as shedding of vortices. Sled vibrations, however, are increased by the disturbances produced by the rails and, during the braking period, by the braking device. Therefore, much effort is being spent to straighten and smooth the rail to an extreme degree of perfection. The master rail, i.e., the western rail, is aligned with an accuracy of .005 inch (.127 mm) tolerance; the eastern rail with .01 inch (.254 mm). But, since absolute straightness will never be obtained, and since typical disturbance patterns become developed even on straight rails, the problem still remains to provide the sled with such dynamic characteristics that it has a minimum response to rail- or brake-induced disturbances. In the following analysis the rails are considered to be perfectly straight.

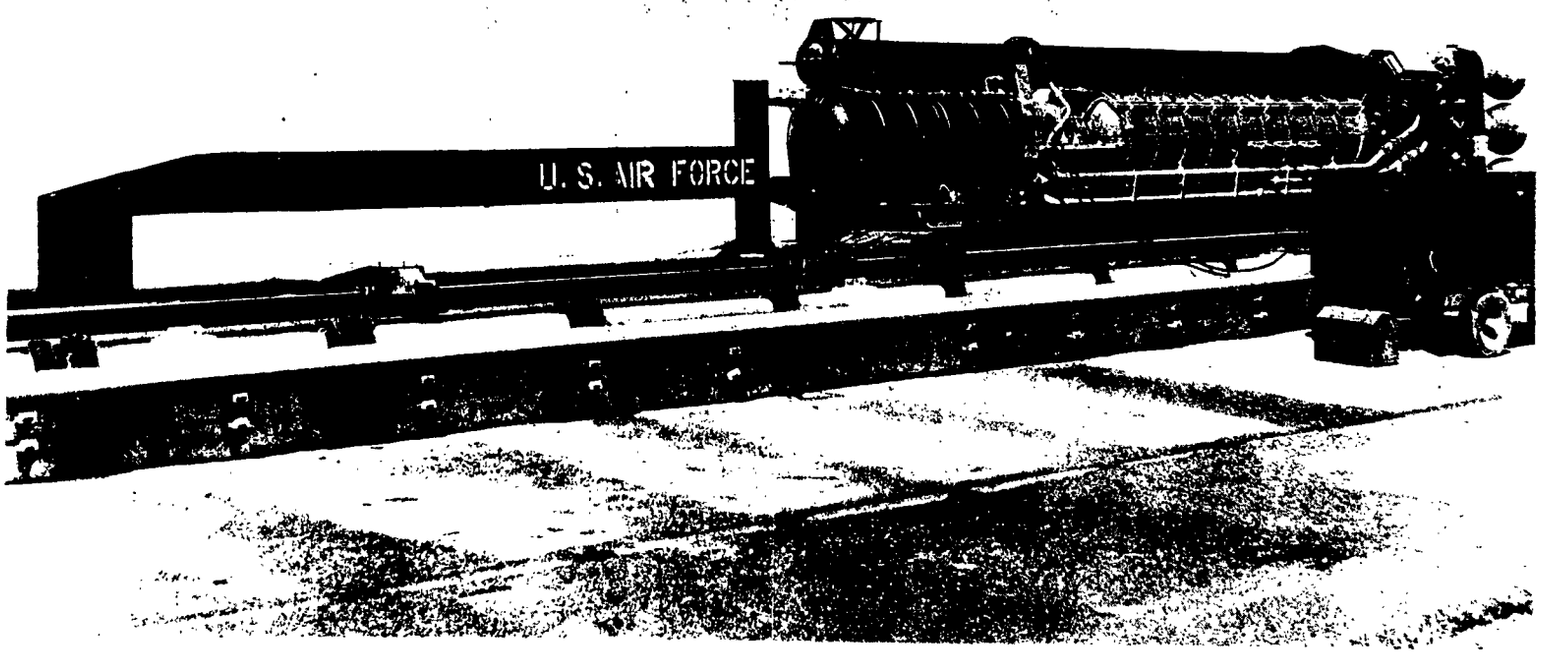

FIGURE 3. SLED CONFIGURATION CONSISTING OF A PUSHER AND FOREBODY

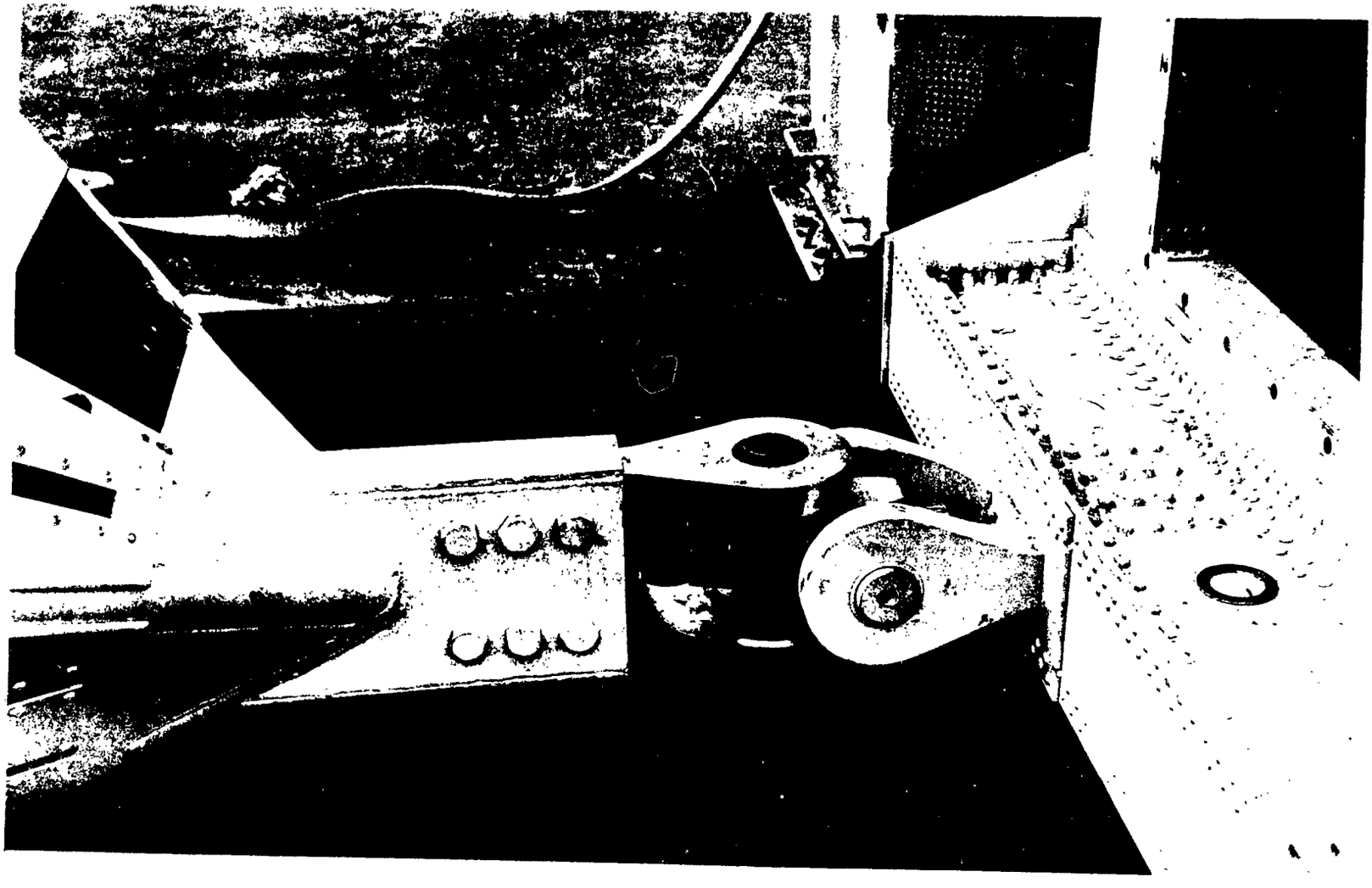

FIGURE 4. COUPLING POINT BETWEEN PUSHER AND FOREBODY

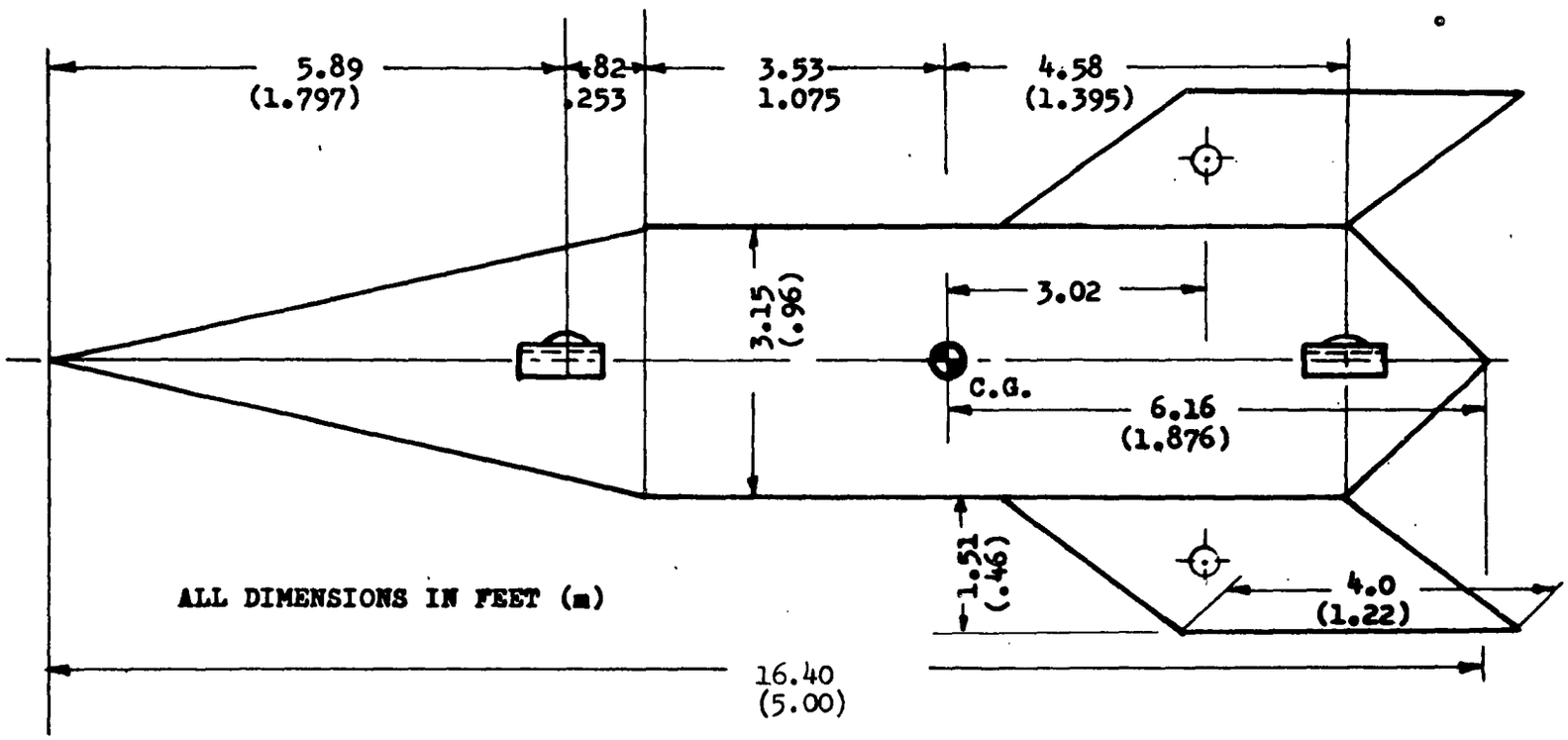

	PHYSICAL CONSTANTS	
WEIGHT	1120 lb	(507.5 kg
MASS	34.81 lb ft^{-1} sec^2	(51.8 kg m^{-1} sec^2)
MOMENT OF INERTIA I_z	850 lb ft sec^2	(117.5 kg m sec^2)
SPRING CONSTANTS		
FRONT SLIPPER BEAM K_F	2×10^6 lb ft^{-1}	(2.975×10^6 kg m^{-1})
REAR SLIPPER BEAM K_R	4×10^6 lb ft^{-1}	(5.95×10^6 kg m^{-1})
RAIL GAGE	7.0 ft	(2.134 m)

FIGURE 5. DIMENSIONS AND PHYSICAL CONSTANTS OF THE INVESTIGATED SLED CONFIGURATION

III. SLED DYNAMICS

This study is primarily concerned with the dynamic behavior of the forebody only. In the following, the word "sled" refers to this portion of the sled team.

The sled configuration selected for the analysis consists of a fin-stabilized axisymmetric body supported by four elastic beams (Fig. 5). At the end each beam is equipped with a slipper used to guide the sled on the rails.

The forces considered instrumental in the description of the sled motion are as follows:

1. The thrust surplus $T^* = T - D_S$, exerted by the pusher in a direction parallel to the rails.(1)

2. The rail induced cross forces $S_1, \ldots S_4$ acting in a direction normal to the rails.

3. The aerodynamic side force Y, composed of forces acting on the axisymmetric portion of the sled and on the vertical tailplanes. Explicitly, a drag force was not introduced. It was assumed that this component of the pressure and friction forces always passes through the center of gravity of the sled and is balanced at every instant by a corresponding fraction of the thrust force. The thrust, in turn, is assumed adjustable in such a way as to neutralize the drag at each

(1) This is an approximation. Actually, the thrust force has the direction of the acceleration of the coupling point between the pusher and the forebody, so that the consideration of a coupled system of pusher and forebody would be more appropriate within the frame of a comprehensive study. For this simplified treatment of the motion, however, the assumption that the thrust vector is always parallel to the rails appears sufficient and more revealing.

instant and, in addition, to generate a specified velocity profile with constant slopes of +8, 0 and - 8 g's (Fig. 6). This velocity profile deviates from that of a standard sled run (Fig. 7); on the other hand, by confining the motion to specified kinematic conditions, the analysis became simplified. All forces considered are confined to the plane of the four slippers which also passes through the center of gravity of the sled. This simplification eliminates roll effects, often observable in practical cases, but still leaves enough important and interesting nonlinear phenomena. Finally, it was assumed that the run occurs on a calm day and there is no feedback of the x-forces between forebody and pusher sled. The balance of forces in y-direction yields:

$$m\ddot{y} = \sum F_y$$

$$= Y + S_1 + S_2 + S_3 + S_4$$

$$= c_{y_\beta} \frac{\rho}{2} U^2 D^2 + S_1 + S_2 + S_3 + S_4 \qquad (1)$$

In this equation the following notations are used:

m	mass of the sled
y	displacement of the c.g. of sled in y-direction
ρ	air density
$U = U(t)$	velocity of the sled in direction of positive x-axis (along the rails)
D	rail gage
β	angle of yaw of the sled
c_{y_β}	derivative of the side force coefficient, c_y of the sled with respect to β
Y	aerodynamic cross force
S_1, S_2, S_3, S_4	cross forces on the slippers, positive in direction of positive y-axis

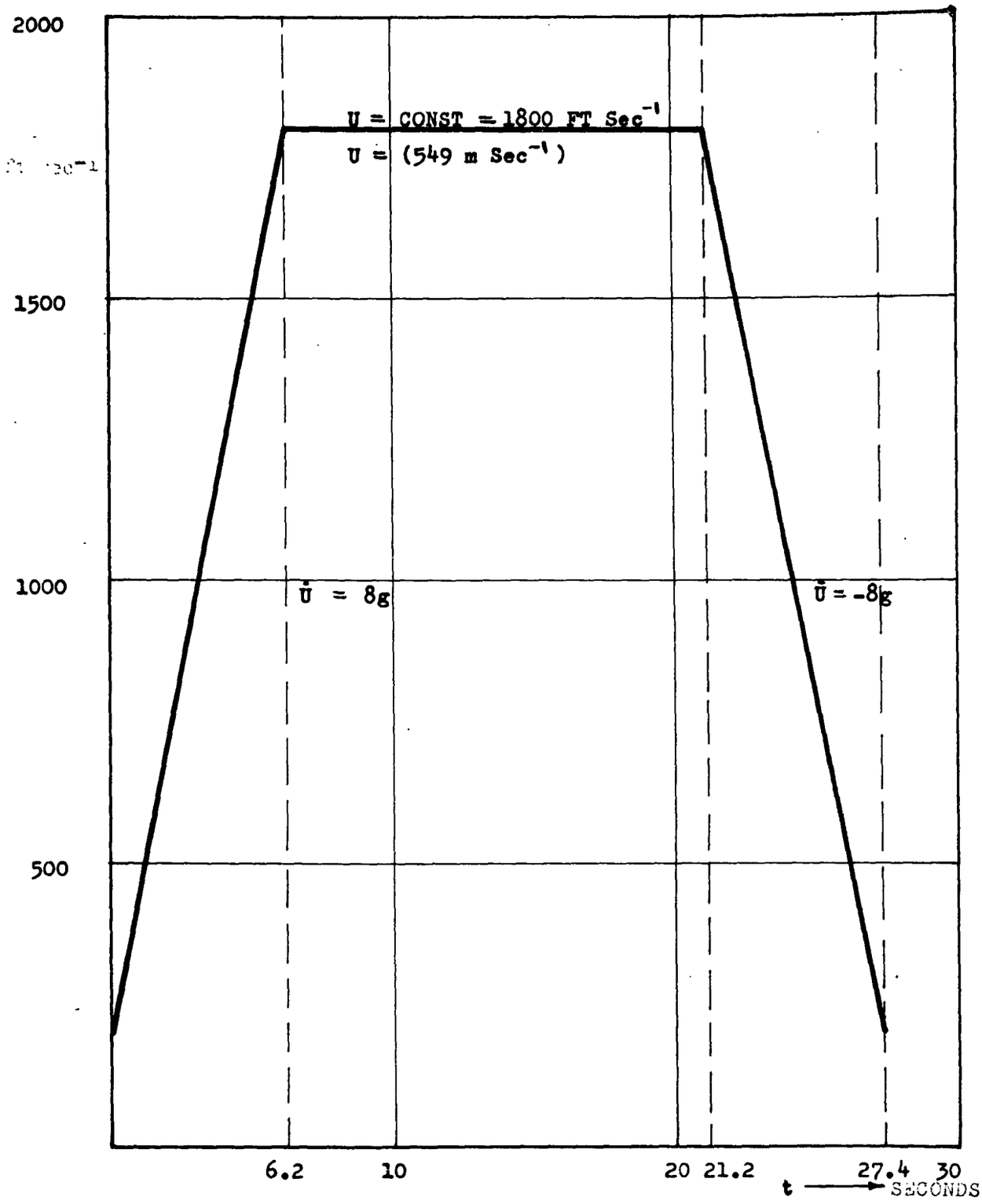

VELOCITY PROFILE SIMULATED ON THE COMPUTER FOR THE STUDY OF THE SLED MOTION

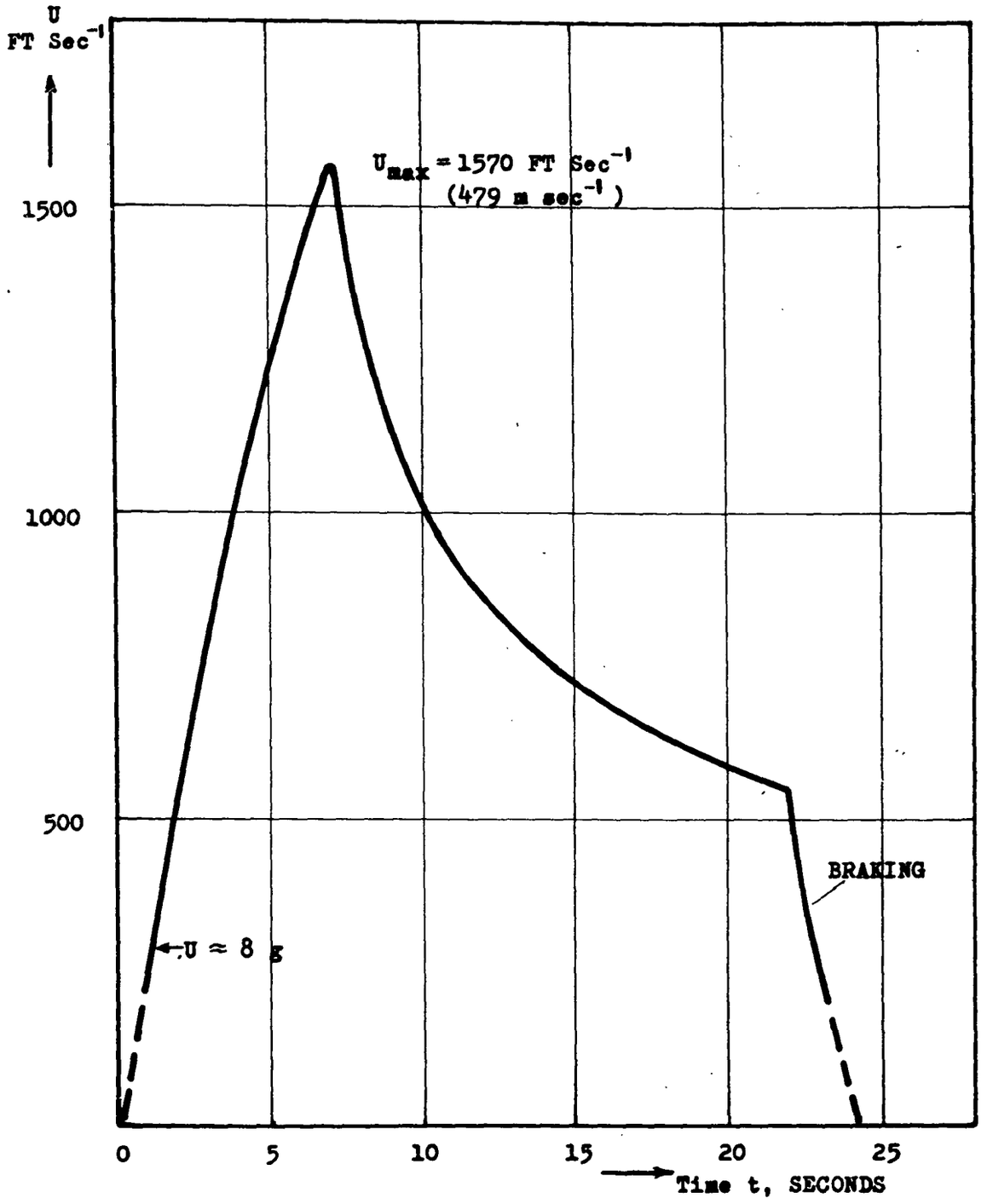

FIGURE 7. VELOCITY PROFILE FOR A GIVEN PUSHER - FOREBODY CONFIGURATION

It is assumed, in general, that the aerodynamic force, Y, is proportional to the dynamic pressure

$$q = \frac{\rho}{2} U^2 ,$$

and is a linear function of the angle of yaw, β. The force is expressed in terms of a side force coefficient c_y, reflecting, in essence, the effects of sled geometry. The variation of c_y with Mach and Reynolds number is disregarded. The equation

$$c_y = \frac{\partial c_y}{\partial \beta} \beta \tag{2}$$

was used to describe the linearized side force effects where the angle of yaw, β, is given by the relation

$$\beta = \psi - \frac{\dot{y}}{U} . \tag{3}$$

In equation (3) ψ denotes the heading angle of the sled, i.e., the angle between its longitudinal axis and the x-orientation, $U = U(t)$ is the velocity of the sled in x-direction, and $\dot{y}$ is the cross-velocity of the sled.

The slipper forces $S_1 \ldots S_4$ depend upon the elastic properties of the slipper beams and can be expressed in terms of the slope K of the $S = f(\epsilon)$ curves, displaying the relationship between the side force S and the slipper displacement ϵ. The slopes of the forces generated on the front slipper beams were assumed to be equal for the two front beams but different from those of the rear slipper beams. The slopes (spring constants) were designated K_F and K_R, respectively. Figure 8 is a schematic representation of these forces.

TOP VIEW

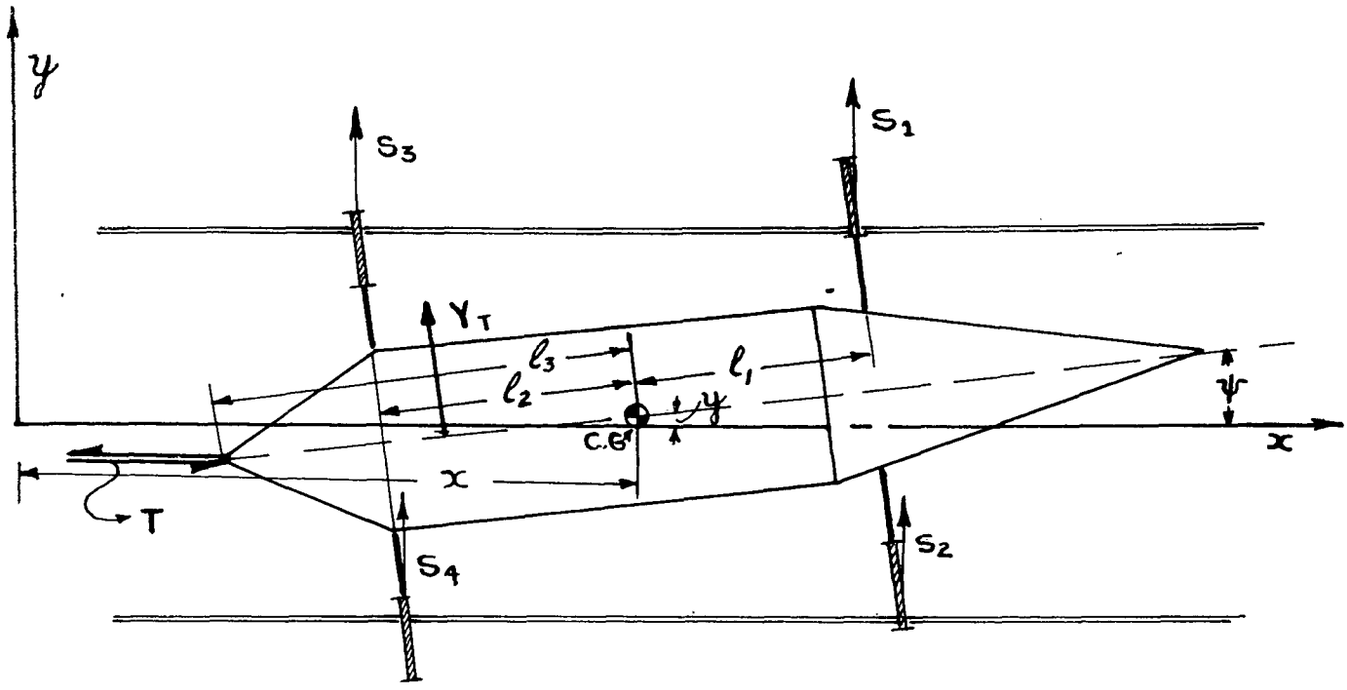

FRONT VIEW

Sled centered on rails.

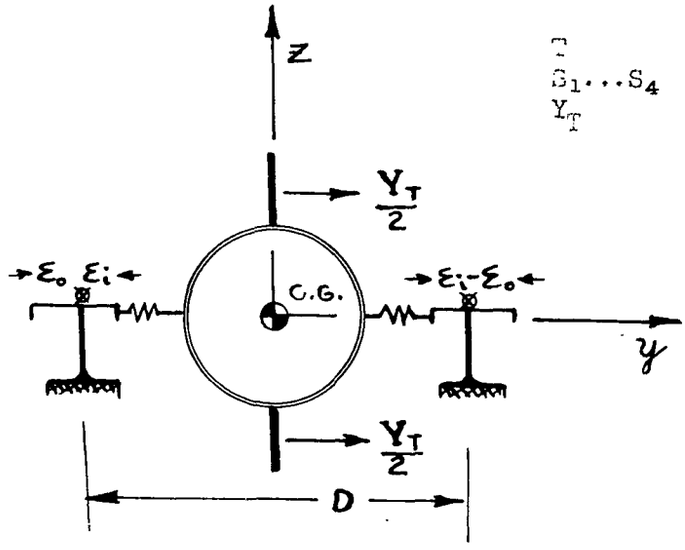

T - Thrust
$S_1 \ldots S_4$ - Slipper cross force
Y_T - Side force induced on tailplane

D - Rail gage

FIGURE 1. THE COORDINATE SYSTEM AND THE SYSTEM OF FORCES ACTING ON THE SLED

The nonlinear variation of the slipper forces $S_1 \ldots S_4$, when plotted as a function of the displacement, ϵ, is caused by the play, ϵ, which must be provided to insure a proper gliding of the sled on the rails. Within the frame of this study it was assumed that the total play, ϵ_t, has an inner part, ϵ_i, of equal magnitude for all four slippers and an outer part, ϵ_o ($\epsilon_o \geq \epsilon_i$), also the same on all four slippers. When ϵ_i's and the ϵ_o's for all slippers are respectively equal, the c.g. of the sled is exactly on the middle of the rails and the sled longitudinal axis coincides with the abscissa of the $x - y$ coordinate system.

The displacement of the slippers, ϵ, can be expressed in terms of the displacement, y ,of the c.g. of the sled and the heading angle, ψ. Inspection of Figure 9 yields the relations:

$$\epsilon_1 = y + \ell_1 \sin \psi - \frac{D}{2}(1 - \cos \psi)$$

$$\epsilon_2 = y + \ell_1 \sin \psi + \frac{D}{2}(1 - \cos \psi)$$

$$\epsilon_3 = y - \ell_2 \sin \psi - \frac{D}{2}(1 - \cos \psi)$$

$$\epsilon_4 = y - \ell_2 \sin \psi + \frac{D}{2}(1 - \cos \psi) \qquad (4)$$

Considering that the heading angle ψ is a small quantity ($\psi_{max} < 0.0174$ rad) equation (4) can be linearized. With $\sin \psi \cong \psi$ and $\cos \psi \cong 1$, one obtains:

$$\epsilon_1 = \epsilon_2 \cong y + \ell_1 \psi$$

$$\epsilon_3 = \epsilon_4 \cong y - \ell_2 \psi \qquad (5)$$

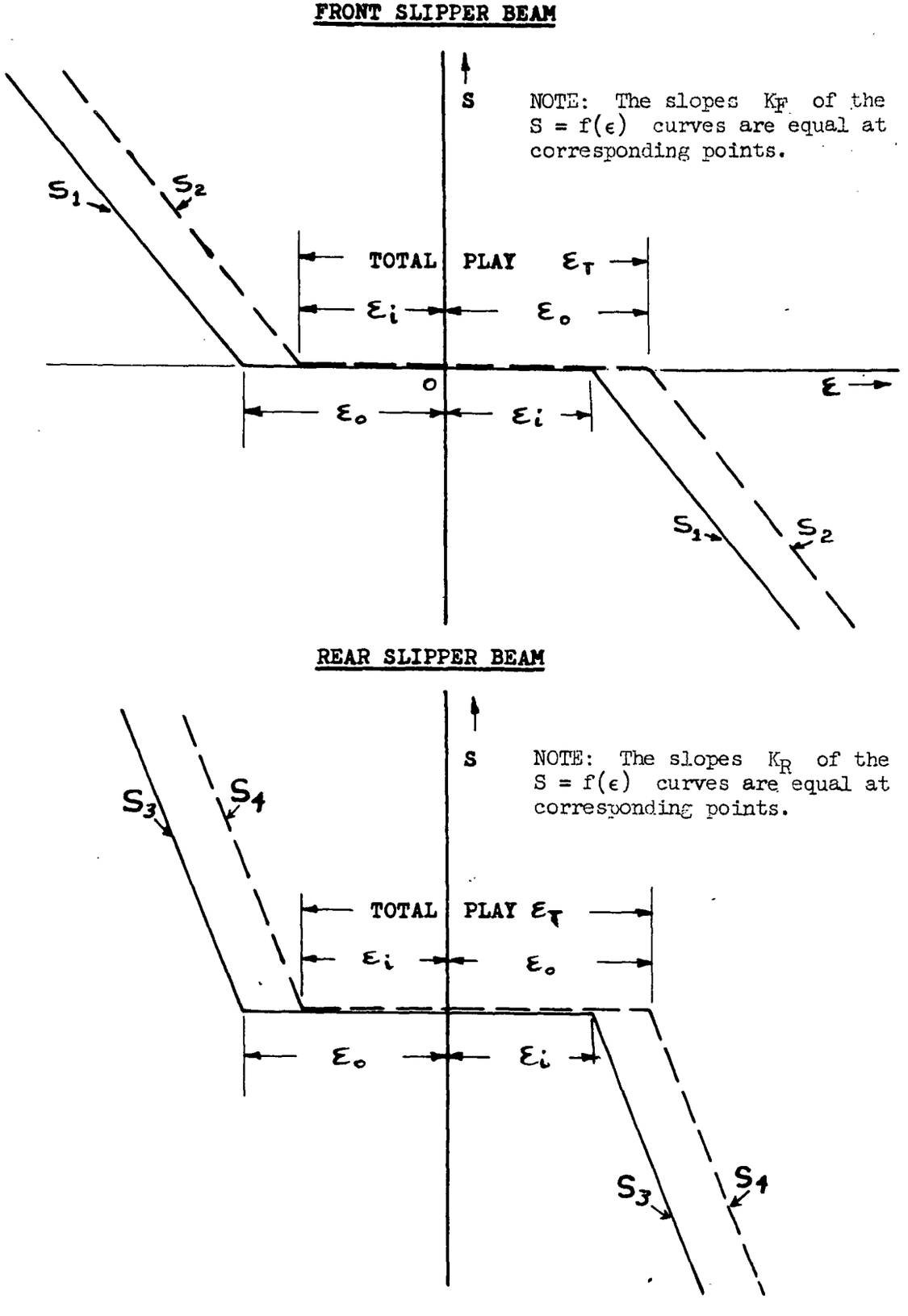

FIGURE 9. **VARIATION OF THE CROSS FORCES $S_1 \ldots S_4$ ON THE SLIPPERS WITH DISPLACEMENT ϵ .**

The yawing motion of the sled is described by the moment equation:

$$I_z \ddot{\psi} = N$$

$$= c_n \frac{\rho}{2} U^2 D^3 + S_1(\ell_1 \cos \psi - \frac{D}{2} \sin \psi)$$

$$+ S_2(\ell_1 \cos \psi + \frac{D}{2} \sin \psi)$$

$$- S_3(\ell_2 \cos \psi + \frac{D}{2} \sin \psi)$$

$$- S_4(\ell_2 \cos \psi - \frac{D}{2} \sin \psi)$$

$$+ T^* \ell_3 \sin \psi \qquad (6)$$

The first term on the right side denotes the aerodynamic moment induced by the lateral and angular displacements of the sled as well as by its rotational velocity; I_z and T^* denote the sled moment of inertia about the z axis and the thrust surplus, respectively. $\ddot{\psi}$ is the angular acceleration of the sled and ℓ_3 is the distance between the coupling point and the c.g. of the sled (Fig. 8).

The slipper forces are nonlinear functions of ϵ_1, ϵ_2, ϵ_3 and ϵ_4, respectively. They are illustrated by Figure 9. The forces are multiplied by the nonlinear functions in the parentheses. Since the yaw angle stays between small limits it was considered sufficiently accurate to replace $\cos \psi$ by one and to neglect $\frac{D}{2} \sin \psi$ in comparison to ℓ_1 and ℓ_2. This reduces the equation (6) to the simpler form:

$$I_z \ddot{\psi} = c_n \frac{\rho}{2} U^2 D^3 + (S_1 + S_2)\, \ell_1 - (S_3 + S_4)\, \ell_2 + T^* \ell_3 \psi \qquad (6a)$$

For small angles the aerodynamic moment of the sled can be thought of as the sum of (1) the moment generated by the side force acting upon the axisymmetric body and (2) the moment produced by side forces on the tail planes of the sled. The tail force, in turn, consists of two parts: one due to the change of the angle of yaw, the other due to the rate of rotation of the sled. We combine the moment generated by the first part of the tail force and the moment induced on the body into one term (since both are functions of the aerodynamic yaw angle β) in that we write for this portion of the total aerodynamic moment

$$
\begin{aligned}
N_1 &= c_{n_1} \frac{\rho}{2} U^2 D^3 \\
&= -\left[\left(\frac{\partial c_y}{\partial \beta}\right)_B \cdot \frac{A_B \, \ell_B}{D^3} + \left(\frac{\partial c_y}{\partial \beta}\right)_T \frac{A_T \, \ell_T}{D^3} \right] \beta \cdot \frac{\rho}{2} U^2 D^3 \\
&= -c_{n_\beta} \beta \frac{\rho}{2} U^2 D^3
\end{aligned} \tag{7}
$$

In this equation the following notations are used:

$\left(\frac{\partial c_y}{\partial \beta}\right)_B$ - the slope of the side force coefficient generated by the body of the sled.

ℓ_B - the distance between the center of pressure and the c.g. of the sled, positive when the center of pressure is located aft the c.g.

$\left(\frac{\partial c_y}{\partial \beta}\right)_T$ - the slope of the side force coefficient generated by the tailplanes

ℓ_T - distance between the center of pressure and the c.g. of the sled, positive when the center of pressure is located aft the c.g.

A_B - reference area of the sled

A_T - area of the tail planes

c_{n_β} - numerical factor describing the static lateral stability of the sled, i.e., the magnitude of the restoring moment per unit angular deflection β

The rate of rotation makes a similar contribution to the tail force as an apparent increase of the angle of yaw. If the sled rotates with the angular velocity $\dot{\psi}$ and the distance between the center of pressure on the tail plane and the center of gravity of the sled is ℓ_T, the lateral velocity component of the tail is equal to $\dot{\psi}\ell_T$. This is equivalent to the change of the angle of yaw of the amount $\dot{\psi}\ell_T U^{-1}$. Thus, the rotation produces a force on the tail plane which is proportional to the angle $\dot{\psi}\ell_T U^{-1}$, and we can write the corresponding moment about the center of gravity of the sled in the form

$$N_2 = c_{n_2} \frac{\rho}{2} U^2 D^3$$

$$= -\left(\frac{\partial c_y}{\partial \beta}\right)_T \frac{A_T \ell_T}{D^3} \dot{\psi}\ell_T U^{-1} \frac{\rho}{2} U^2 D^3$$

$$= -\left(\frac{\partial c_y}{\partial \beta}\right)_T \cdot \frac{A_T \ell_T^2}{D^3} U^{-1} \dot{\psi} \frac{\rho}{2} U^2 D^3 = -c_{\dot{\psi}} \frac{\rho}{2} U^2 D^3 \dot{\psi} \qquad (8)$$

where $c_{\dot{\psi}}$ is a function of the sled velocity U.

Equation (8) describes the damping effect generated by the tailplanes of the sled. A corresponding aerodynamic effect of the angular velocity, $\dot{\psi}$, induced by the sled body, was neglected because of its smallness.

The moment equation (6) can now be written as follows:

$$I_z \ddot{\psi} = -\left[c_{n_\beta} \left(\psi - \frac{\dot{y}}{U}\right) + c_{\dot{\psi}} \dot{\psi}\right] \frac{\rho}{2} U^2 D^3$$

$$+ (S_1 + S_2)\, \ell_1 - (S_3 + S_4)\, \ell_2 + T\, \ell_3\, \psi \qquad (6b)$$

in which the second and third terms on the right-hand side represent the nonlinear variation of the moment caused by the sled displacement y and the heading angle ψ.

Equation (6b) together with equation (1) constitutes a set of simultaneous differential equations of second order, which describes the motion of the sled in the x-y plane.

IV. APPROACH

Even for the idealized cases for which the sled motion has been confined, an analytical treatment of the problem by modern analytical means, known to the authors, appears to be rather involved. Thus, in order to obtain a quantitative appraisal of the various parameters affecting the mode of motion of the sled and its stability, several numerical examples were treated by simulating the sled motion on a PACE analog computer. For practical purposes the numerical accuracy of an analog computer with an estimated error of not more than .5 percent was considered by far sufficient.

Furthermore, the stability of motion was examined for a modified sled configuration, i.e., a system for which the slipper forces can be considered linear functions of displacement.

V. ANALOG COMPUTER PROCEDURES

Standard techniques were used to mechanize the equations of motion on the analog computer. The computer time was chosen to be eight times real time. The summing and integrating amplifiers were of the chopper-stabilized, high precision, D.C. type. The multipliers were all electronic, using the time division principle.

The discontinuities in the displacement-force diagram for the front and the rear slippers were simulated by a pair of amplifiers with diodes in the feedback and input biases, determining the cut-in voltage of the outputs. The summing amplifiers, summing the inputs of a pair of these biased diode amplifiers, will give an output voltage only if the input exceeds the bias in either polarity. Thus, the bias voltage determines the "dead" space which corresponds to the slipper play ϵ. Circuits of this type eliminate the errors due to contact potential of the diodes.

A difficulty encountered in the process of motion simulation consisted in finding a suitable compromise in scaling the very tight spring-force loops and the relatively loose aerodynamic loops. The time scale of eight to one and a gain of approximately 400 for the spring-forces, as they are fed into the integrators for y and β, brought a satisfactory solution. For such high integrator gains a certain amount of drift is inevitable. Physically, this can be interpreted as a moderate side wind.

The computer diagram showing the simulation is given in Figure 10.

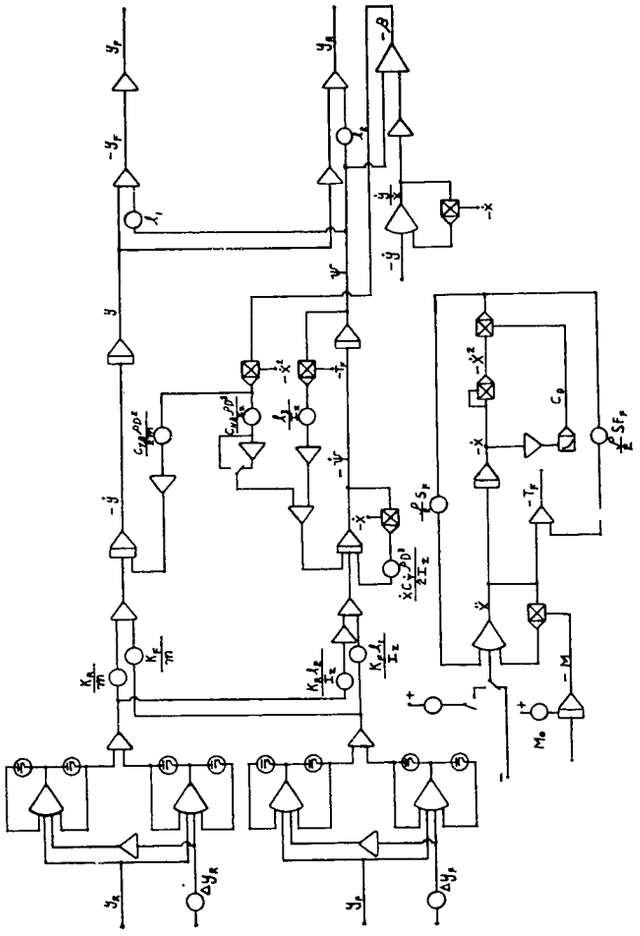

FIGURE 10. SLED MOTION SIMULATION ANALOG COMPUTER DIAGRAM

VI. THE LINEARIZED SYSTEM

For the linearized system the slipper forces $S_1 \ldots S_4$ can be expressed in the following way (see, e.g., equation (5)):

$$S_1 = - K_F' \epsilon_1 = - K_F'(y + \ell_1 \psi)$$

$$S_2 = - K_F' \epsilon_2 = - K_F'(y + \ell_1 \psi)$$

$$S_3 = - K_R' \epsilon_3 = - K_R'(y - \ell_2 \psi)$$

$$S_4 = - K_R' \epsilon_4 = - K_R'(y - \ell_2 \psi) \qquad (9)$$

where K_F' and K_R' denote the modified spring constants.

With

$$Y = \frac{\partial c_y}{\partial \beta} \cdot \frac{\rho}{2} D^2 U^2 \cdot \beta = \frac{\partial c_y}{\partial \beta} \frac{\rho}{2} D^2 (\psi - \frac{\dot{y}}{U}) U^2 = Y_\beta (\psi - \frac{\dot{y}}{U}) U^2$$

$$N_1 = \frac{\partial c_n}{\partial \beta} \frac{\rho}{2} D^3 U^2 \beta = \frac{\partial c_n}{\partial \beta} \frac{\rho}{2} D^3 (\psi - \frac{\dot{y}}{U}) U^2 = N_\beta (\psi - \frac{\dot{y}}{U}) U^2$$

$$N_2 = \frac{\partial c_n}{\partial \dot{\psi}} \frac{\rho}{2} D^3 U^2 \dot{\psi} = N_{\dot{\psi}}' U^2 \dot{\psi} = N_{\dot{\psi}}' \dot{\psi} U^2$$

one obtains the following set of simultaneous differential equations of second order:

$$m \ddot{y} + Y_\beta U \dot{y} + 2 K y + (2 L - Y_\beta U^2) \psi = 0$$

$$I_z \ddot{\psi} - N_{\dot{\psi}}' U^2 \dot{\psi} + \left[2 M - T^* \ell_3 - N_\beta U^2 \right] \psi + N_\beta U \dot{y} + 2 L y = 0 \qquad (10)$$

where

$$K = K_F' + K_R'$$

$$L = K_F' \ell_1 - K_R' \ell_2$$

$$M = K_F' \ell_1^2 + K_R' \ell_2^2$$

the coefficients of the quartic

$$A_4 \lambda^4 + A_3 \lambda^3 + A_2 \lambda^2 + A_1 \lambda + A_0 = 0 \qquad (11)$$

are the following expression

$$A_4 = m I_z$$

$$A_3 = U(Y_\beta I_z - m N_\psi U)$$

$$A_2 = m(2M - T^* \ell_3) + 2K I_z - U^2(m N_\beta + Y_\beta N_\psi U) \qquad (12)$$

$$A_1 = U\left[Y_\beta (2M - T^* \ell_3) - 2K N_\psi U - 2K N_\beta\right]$$

$$A_0 = 2K(2M - T^* \ell_3) - 4L^2 + U^2(2L Y_\beta - 2K N_\beta) \ .$$

The evaluation of the coefficients $A_4 \ldots A_0$ for various values of the spring constant, $K = K_F' + K_R'$ ranging from $K = 6 \times 10^5$ lb ft^{-1} to about $K = 9 \times 10^3$ lb ft^{-1} has shown that the Routh stability conditions

$$A_4; A_3; A_2; A_1; A_0 > 0$$

and (13)

$$A_1(A_3 A_2 - A_4 A_1) - A_3^2 A_0 > 0$$

are fulfilled, indicating a stable system. The numerical values of the various A-coefficients, the resulting natural frequencies of the motion and the damping exponents for a representative configuration with

$$Y_\beta = 0.051 \text{ lb ft}^{-2} \text{ sec}^2 \quad (cy_\beta = 1.0)$$

$$N_\beta = -0.02675 \text{ lb ft}^{-1} \text{ sec}^2 \quad (cn_\beta = -0.075)$$

$$N_\psi = -0.2283 \text{ lb ft}^{-1} \text{ sec}^{-3} \quad (Uc_\psi = -0.64)$$

are compiled in the table on page 27.

VII. RESULTS

Some of the results obtained in the form of computer graphs are displayed in Figures 11 through 13. It should be noted that, for purposes of simplification, the assumption of equal inner and outer play components ($\epsilon_i = \epsilon_o = \epsilon$) was used throughout the study. Thus, whenever the front or the rear beam of the sled becomes engaged with the rails (because of a lateral displacement or a rotation of the sled) both halves of the pertinent beam were equally stressed. It is possible, therefore, to substitute for the spring constants of the two halves of the front beam, a "combined" spring constant, K_F, and for those of the rear beam a corresponding constant, K_R.

To alleviate comparison, six computer graphs, each of them representing a complete sled run of about 27.4 seconds duration, are assembled in one figure. Each graph displays eight variables which characterize the lateral motion of the sled and their variation with time, t. Plotted are from top to bottom:

1. $y_F = y_F(t)$ — the lateral displacement of the end point of the front beam, if rigid
2. $y_R = y_R(t)$ — the lateral displacement of the end point of the rear beam, if rigid

3.	$y_{c.g.} = y_{c.g.}(t)$	the lateral displacement of the c.g. of the sled
4.	$\beta = \beta(t)$	the yaw angle of the sled
5.	$\dot{y} = \dot{y}(t)$	the lateral velocity component of the c.g. of the sled
6.	$\dot{\psi} = \dot{\psi}(t)$	the angular velocity of the sled
7.	$S_R = S_R(t)$	the force acting on the rear end of the sled
8.	$S_F = S_F(t)$	the force acting on the front end of the sled

The time scale is displayed at the bottom of the graphs, each unit representing one-eighth of a second. (As mentioned before, the computer time was chosen eight times real time; thus a sled run of 27.4 seconds duration is composed of $27.4 \times 8 = 219.2$ units, i.e., requires about 220 seconds on the computer.)

For a period of about 6.22 seconds ($\sim$ 50 units) the sled was subjected to a constant acceleration of 8 g's which produces a velocity increment of $\Delta U \approx 1600$ ft sec^{-1}. In the study, all sled runs started with an initial velocity of $U_o = 200$ ft sec^{-1} (to avoid computational difficulties as the computer had to evaluate expressions containing the sled velocity in the denominator) so that, at the end of the acceleration period, the velocity of the sled had reached the value $U = 1800$ ft sec^{-1}. (Fig. 6) For about 15 seconds (120 units) this velocity was held constant; then by applying a negative acceleration of -8 g's the sled was decelerated until its velocity had reached the 200 ft sec^{-1} mark.

The upper row of computer graphs in Figure 11 displays three sled runs in which the slipper play, ϵ, was varied from $\epsilon = .0013$ ft to $\epsilon = .0039$ ft while the aerodynamic coefficients, c_{y_β}, c_{n_β} and $Uc_{\dot{\psi}}$ as well as the spring constants K_F and K_R were held constant ($2K_F = K_R = 4 \times 10^5$).

TABLE

	U ft sec^{-1} T* lb		500 9973	1000 13011	1500 18074	1500 9114
$c_{y\beta} = 1.0$; $c_{n\beta} = -.075$ $Uc\dot{\psi}' = -.64$ $2K_F' = K_R' = 4 \times 10^5$	$A_4 \times 10^{-4}$	lb^2 sec^4	2.958	2.958	2.958	2.958
	$A_3 \times 10^{-4}$	lb^2 sec^3	2.5648	5.1295	7.6943	7.6943
	$A_2 \times 10^{-8}$	lb^2 sec^2	1.8655	1.8655	1.8656	1.8676
	$A_1 \times 10^{-8}$	lb^2 sec^1	7.3012	14.5928	21.8654	21.9083
	$A_0 \times 10^{-13}$	lb^2	2.5428	2.5356	2.5236	2.5304
	ω_1	sec^{-1}	207.7	208.0	208.4	208.4
	ω_2	sec^{-1}	141.2	140.8	140.2	140.3
	n_1	cps	33.06	33.10	33.16	33.17
	n_2	cps	22.47	22.41	22.31	22.33
	ν_1	sec^{-1}	-.2740	-.5477	-.8208	-.8197
	ν_2	sec^{-1}	-.1595	-.3193	-.4798	-.4809
$c_{y\beta} = 1.0$; $c_{n\beta} = -.075$ $Uc\dot{\psi}' = -.64$ $2K_F = K_R = 4 \times 10^4$	$A_4 \times 10^{-4}$	lb^2 sec^4	2.958	2.958	2.958	2.958
	$A_3 \times 10^{-4}$	lb^2 sec^3	2.5648	5.1295	7.6943	7.6943
	$A_2 \times 10^{-8}$	lb^2 sec^2	1.8486	1.8489	1.8500	1.8484
	$A_1 \times 10^{-7}$	lb^2 sec^1	7.1652	14.2352	21.1318	21.5430
	$A_0 \times 10^{-11}$	lb^2	2.4616	2.3897	2.2697	2.3370
	ω_1	sec^{-1}	65.77	66.51	67.64	66.97
	ω_2	sec^{-1}	43.86	42.73	40.95	41.96
	n_1	cps	10.47	10.59	10.77	10.66
	n_2	cps	6.98	6.80	6.52	6.68
	ν_1	sec^{-1}	-.2765	-.5503	-.8207	-.8048
	ν_2	sec^{-1}	-.1570	-.3167	-.4798	-.4958
$c_{y\beta} = 1.0$; $c_{n\beta} = -.075$ $Uc\dot{\psi}' = -.64$ $2K_F = K_R = 4 \times 10^3$	$A_4 \times 10^{-4}$	lb^2 sec^4	2.958	2.958	2.958	2.958
	$A_3 \times 10^{-4}$	lb^2 sec^3	2.565	5.130	7.694	7.694
	$A_2 \times 10^{-7}$	lb^2 sec^2	1.667	1.683	1.692	1.887
	$A_1 \times 10^{-6}$	lb^2 sec^1	5.755	10.556	13.448	17.743
	$A_0 \times 10^{-9}$	lb^2	1.649	0.929	-0.27	0.404
	ω_1	sec^{-1}	20.86	22.49	Unstable	24.77
	ω_2	sec^{-1}	11.32	7.88		4.69
	n_1	cps	3.32	3.58		3.94
	n_2	cps	1.80	1.25		.75
	ν_1	sec^{-1}	-.2976	-.5865		-.8429
	ν_2	sec^{-1}	-.1358	-.2806		-.4577

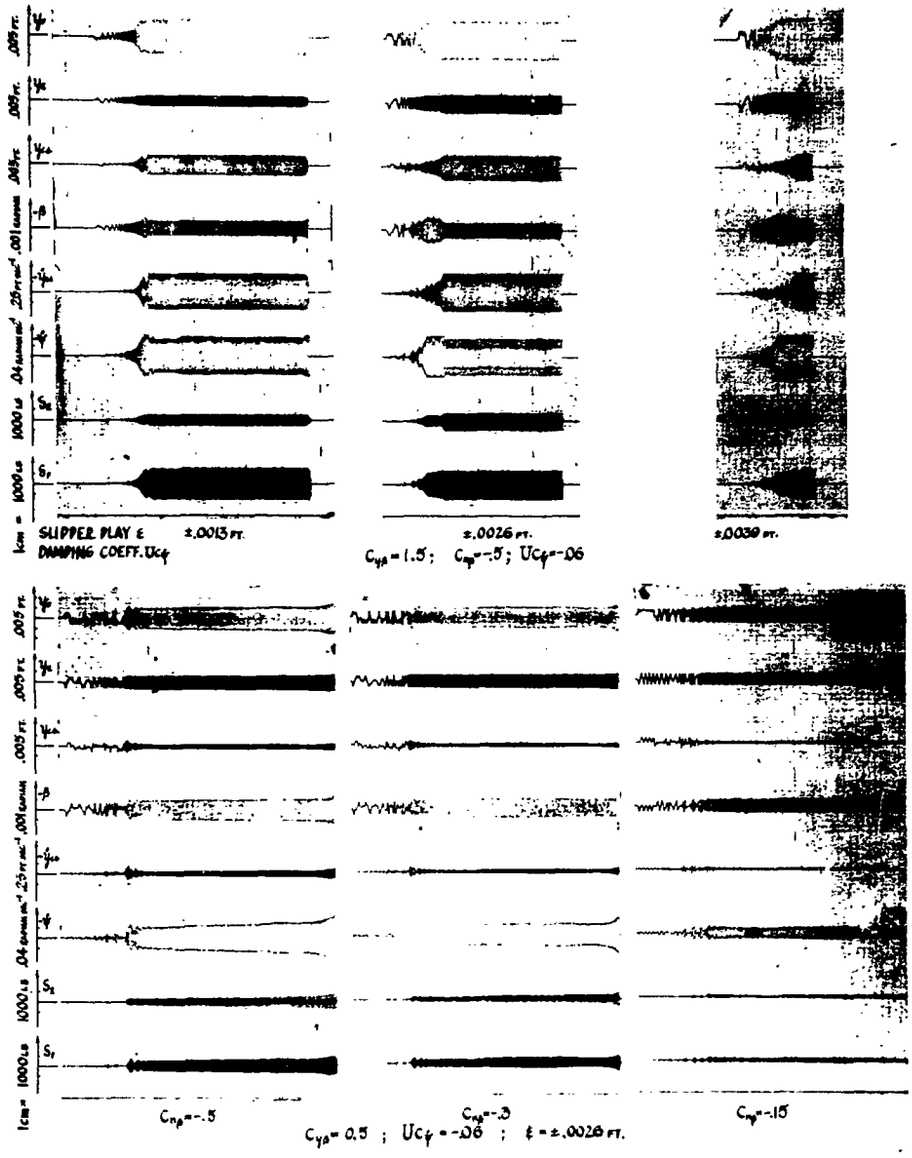

FIGURE 11. VARIATION OF THE SLED MOTION PARAMETERS WITH TIME

Spring Constants: $2 K_F = K_R = 4 \times 10^5$ lb ft^{-1}

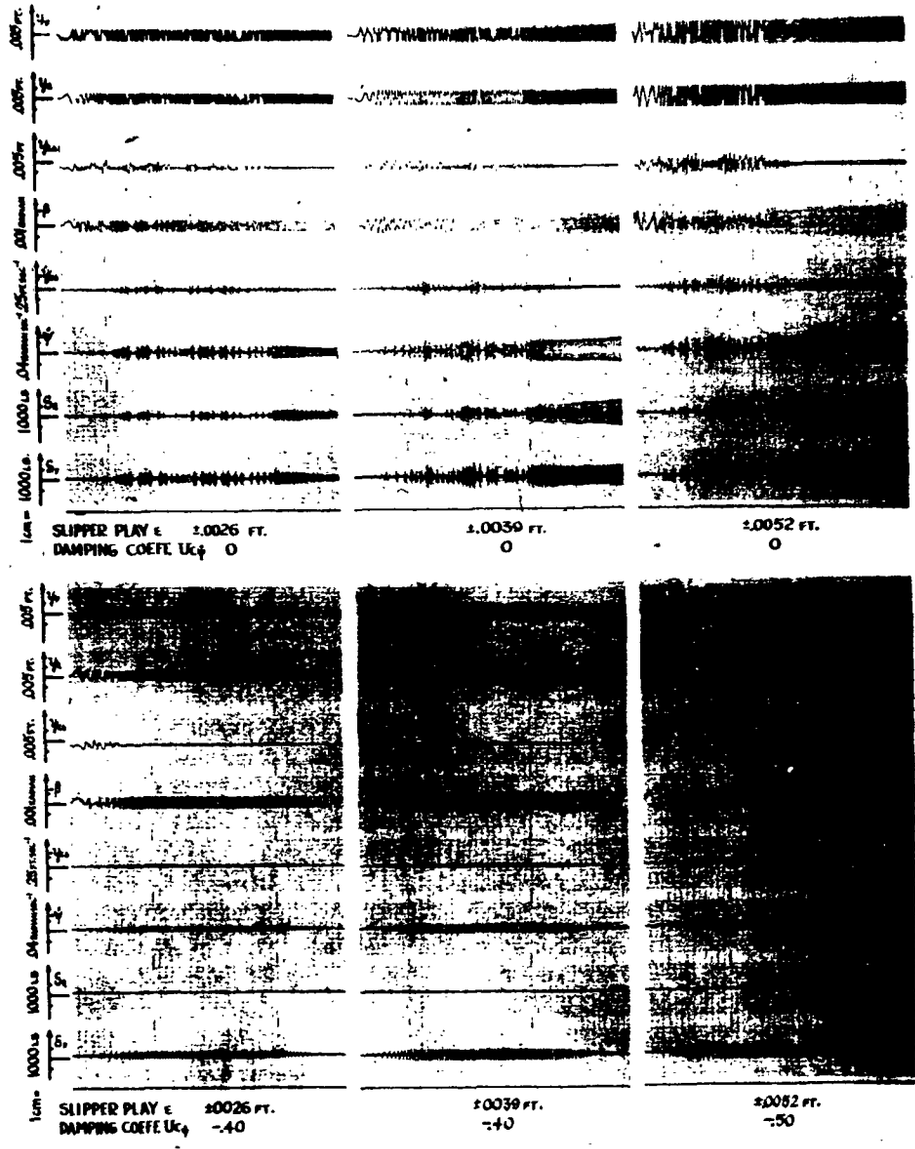

FIGURE 12. VARIATION OF THE SLED MOTION PARAMETERS WITH TIME

Spring Constants: $2K_F = K_R = 2 \times 10^6$ lb ft^{-1}, $C_{y\beta} = .5$; $C_{n\beta} = -.075$

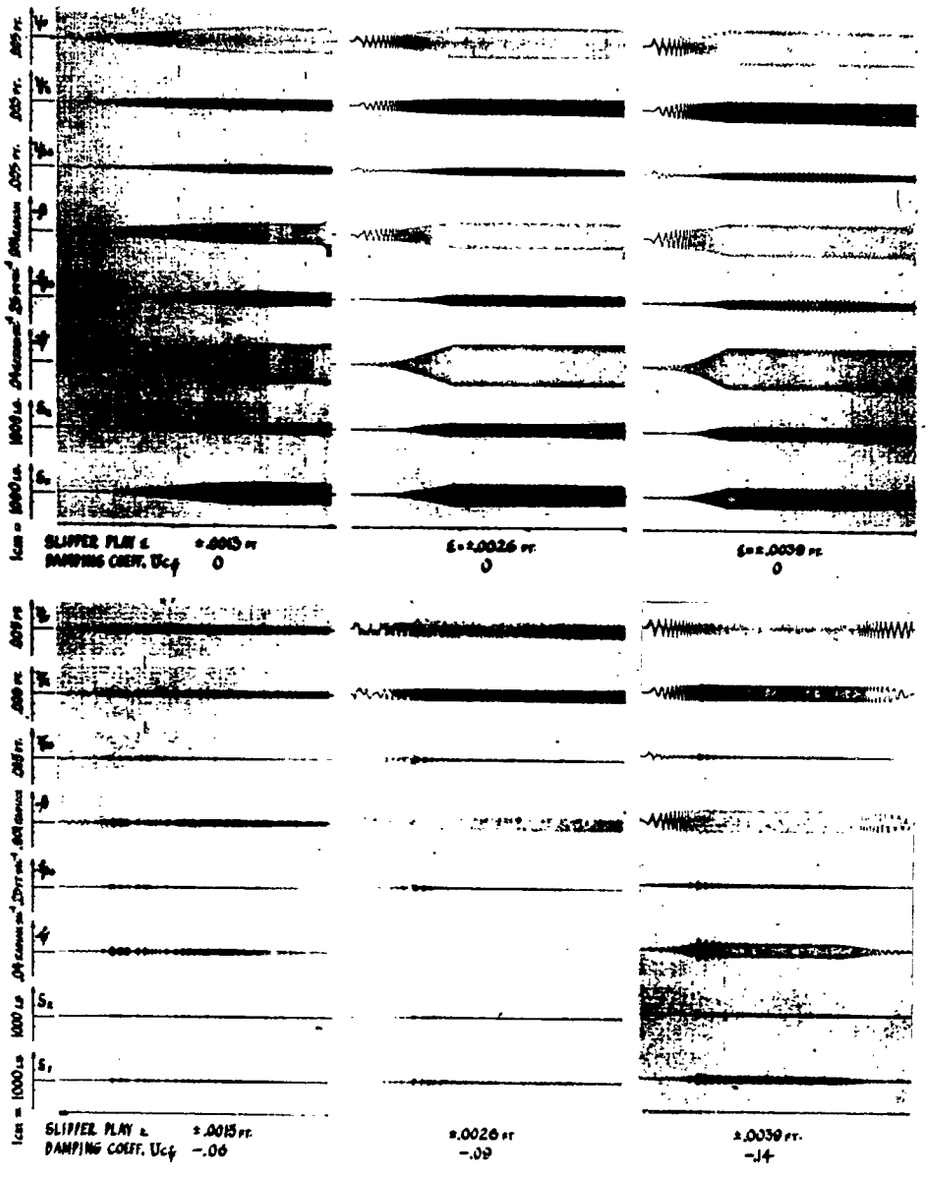

FIGURE 13. VARIATION OF THE SLED MOTION PARAMETERS WITH TIME

Spring Constants: $2K_F = K_R = 4 \times 10^5$ lb ft^{-1}; $C_{y\beta} = .5$; $C_{n\beta} = -.075$

It can be noted that a periodic motion becomes established as soon as the sled reaches the U = const portion of the run. Nearly all motion variables exhibit high upper limits. Comparing the graphs from left to right, it can be seen that with increasing slipper play a gradual increase of the amplitude of the displacement, y_F, takes place. Remembering that y_F represents the total displacement of the front beam (i.e., the play, ϵ, and the deflection of the spring, $S_F K_F^{-1}$) its magnitude is not indicative of the elastic force, S_F, which is proportional to the difference $\Delta = y_F - \epsilon$. Thus, the recorded gradual reduction of S_F with increasing ϵ does not contradict the above described behavior of the displacement y_F.

On the other hand, the variation of the forces, S_R, exerted on the rear beam, with ϵ is different; these forces first increase with increasing ϵ, but they become smaller as ϵ is further increased. The examination of the graphs shows that this behavior is related to the mode of motion of the sled. In the first two graphs the motion can, perhaps, be described as a rotation about a "point" located several feet behind the rear beam of the sled, the distance increasing with increasing ϵ. In the third graph, however, the "point" of rotation is shifted forward and is now lying between the c.g. and the rear beam. Thus, the instantaneous forces exerted on the front and the rear beams which in the first two cases had equal signs are now acting in opposite direction.

Finally, it can be noted that with increasing slipper play, ϵ, a considerable reduction of the dominant frequency is taking place. ($n \cong 14$ cps for $\epsilon = .0013$ ft as compared to $n \cong 10.5$ for $\epsilon = .0039$ ft)

The lower row of Figure 11 displays the behavior of the motion variables for a constant value of the slipper play ϵ ($\epsilon = .0026$ ft). In this arrangement the coefficient of the aerodynamic moment, $c_{n\beta}$, was varied from $-.5$ to $-.15$ while $c_{y\beta}$ and Uc_{ψ} were held constant. The meaning of this is that the center of pressure of the aerodynamic load

was shifted from a position at a distance of 7 feet aft the c.g. (hypothetical case) to a position 2.1 feet aft the c.g. of the sled. It can be observed that with decreasing distance a gradual reduction of forces and corresponding frequencies takes place.

Figure 12 displays the effects of damping for various values of the slipper play ϵ. The spring constants are chosen to be five times larger than those in the previous case. The aerodynamic coefficients selected for this configuration are those of the representative sled shown in Figure 5 ($c_{y\beta} = .5$; $c_{n\beta} = -.075$). The upper row of graphs displays the motion of a sled for which the damping coefficient is assumed to be zero, while the lower row exhibits a configuration having a moderate damping coefficient ($Uc_{\dot{\psi}} = -.40$ to $-.50$). The benefits obtained by damping are obvious. It is interesting to note the distinct variation of forces exerted on the front and the rear beam with damping; while for $Uc_{\dot{\psi}} = 0$, the forces on the front and the rear beam are nearly equal, a moderate damping coefficient of about $-.4$ to $-.5$ causes the spring forces on the rear beam practically to disappear.

The comparison of the frequencies of the sled runs in the upper row with those on the lower row, shows that damping also causes a substantial reduction of the dominant frequency, n; the n-values decrease from about 7.8 cps (upper row) to about 3.5 (lower row).

Figure 13 displays the effects of damping for a sled equipped with softer springs ($K_F = 2 \times 10$ lb ft^{-1}; $K_R = 4 \times 10^5$). Here again the benefits resulting from a properly selected damping coefficient are recognizable. It should be noted, however, that a sled equipped with softer slipper beams is more susceptible to the magnitude of the slipper play ϵ, than a sled with stiffer beams. While for $\epsilon = .0013$ foot the slipper forces on the front beam are exceptionally small ($S_F = 135$ lb; $S_R = 65$ lb) their magnitude increases continually with increasing slipper play. ($S_F = 315$ lb; $S_R = 100$ lb for $\epsilon = .0039$ ft)

To obtain a better insight into the details of the sled motion the time scale in Figure 14 was expanded. The two computer graphs shown represent the first portion of the sled run, i.e., the acceleration phase and the beginning of the U = const phase. It can be noted that the displacements y_F and y_R have opposite signs; every time the front beam moves upward the rear beam moves downward. The displacement of the c.g. of the sled is relatively small. The motion can be described as a rocking of the sled about a "point" located in the neighborhood of the c.g. of the sled. Actually, the "point" is a relatively small area to which the instantaneous center of rotation is confined and in which the center is following a complicated path. However, in the first approximation the area can be regarded as a "point" about which the sled is oscillating.

The path described by the end point of the rear beam is nearly a sinusoid with an amplitude which is smaller than the slipper play, ϵ. No elastic forces are exerted on the rear beam. Thus, the sled can be regarded as a rigid body with elastic forces acting on its front end in intervals whenever the slipper stops are touching the rails, and with a periodic aerodynamic force with its center located 1.05 feet aft the c.g.

A detailed analysis of the recorded modes of motion of the sled could not be carried out as time was pressing and only a very limited number of computer graphs, suitable for an analysis, was available to the authors at the time of this writing.

The variation of the slipper forces S and of the dominant frequency n with slipper play ϵ is shown on Figures 15 and 16, respectively. The spring constants and the aerodynamic coefficients were held constant (see Fig. 15 and 16). Details of the sled motion which correspond to these charts are presented in the upper row of Figure 11. It can be noted that for smaller ϵ's a gradual reduction of the slipper forces on the front beam and an increase of forces on the rear beam takes place with increasing ϵ. This behavior is

characteristic of that mode of sled motion for which the center of rotation is located aft the rear beam. As soon as the motion pattern changes (the center of rotation being located between the front and the rear slipper beam) a considerable reduction of the rear slipper forces can be observed.

Extrapolating the measured frequencies (Fig. 16) toward $\epsilon = 0$ one finds that with no slipper play the sled will oscillate with the frequency n of about 15.9 cps. A frequency of 15.91 cps was obtained analytically by assuming that a rigid body, having a mass and an inertia moment corresponding to that of the sled, is supported by two springs with constants of the same magnitude as those of the sled. The observed shape of the sled motion which corresponds to the frequency of 15.9 cps is the second natural mode of the oscillating body (lower frequency, center of rotation located aft the c.g.).

Figures 17,18 and 19 show the effects of damping for various values of the slipper play ϵ and of the spring constant K. It can be seen that in practically all cases a considerable reduction of the slipper forces on the front and on the rear beam takes place. It should be kept in mind, however, that the true aerodynamic coefficients may be substantially lower than the values assumed in this study. In the β-near-zero range the boundary layer might have an adverse effect on the sensitiveness of the sled to small angular deflections, thus reducing the magnitude of the aerodynamic coefficients.

Figure 20 shows the variation of the slipper forces S with spring stiffness K for various values of the slipper play ϵ. The mode of motion of the sled was that for which the center of rotation is located between the slipper beams. It appears that by proper adjustment of the slipper play ϵ and of the spring stiffness K, the slipper forces can be minimized.

Figure 21 shows the variation of the dominant frequency, n, with the spring stiffness, K, the slipper play, ϵ, being the parameter. It can be noted that larger frequency changes take place only in the range of lower spring stiffness, K. At higher K's only minor changes in n can be observed. The mode of motion of the sled is the same as that of Figure 20. For comparison purposes the variation of the frequencies of the undamped sled configuration was also included.

VIII. CONCLUSIONS

The results presented indicate that the simulation of a rocket sled motion on an analog computer exhibits the possibility of being efficient in the attempt to understand the mechanism of the sled motion. Through the use of this technique some tedious computational difficulties could be avoided and the analysis of the dynamic properties of a sled simplified.

The method provides answers on the influence of various parameters on the behavior of the sled, thus permitting conclusions regarding their optimization.

The data presented herein must be considered preliminary as only a limited number of cases were examined.

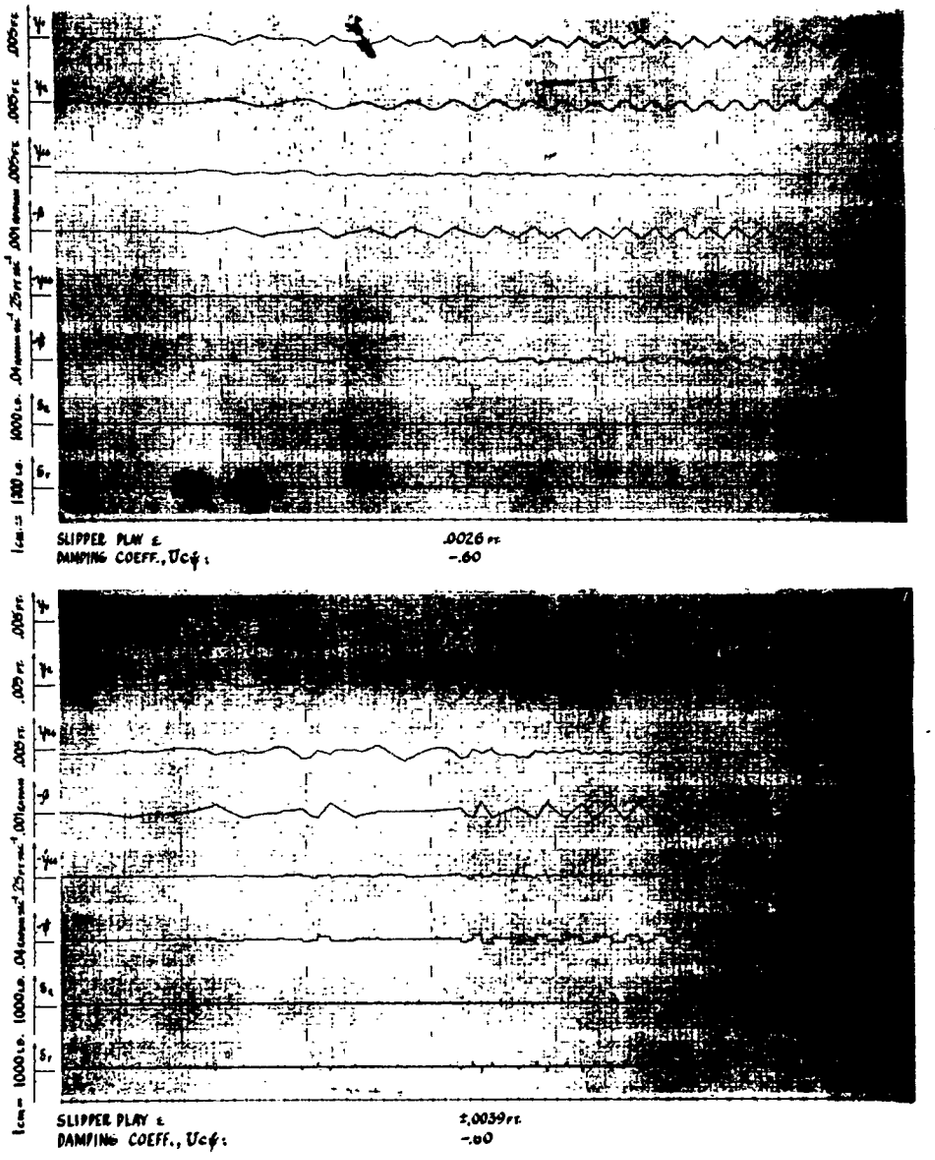

FIGURE 14. VARIATION OF THE SLED MOTION PARAMETERS WITH TIME

Spring Constants: $2K_F = K_R = 2 \times 10^6$ lb ft^{-1}; $C_{y\beta} = .5$; $C_{n\beta} = -.075$

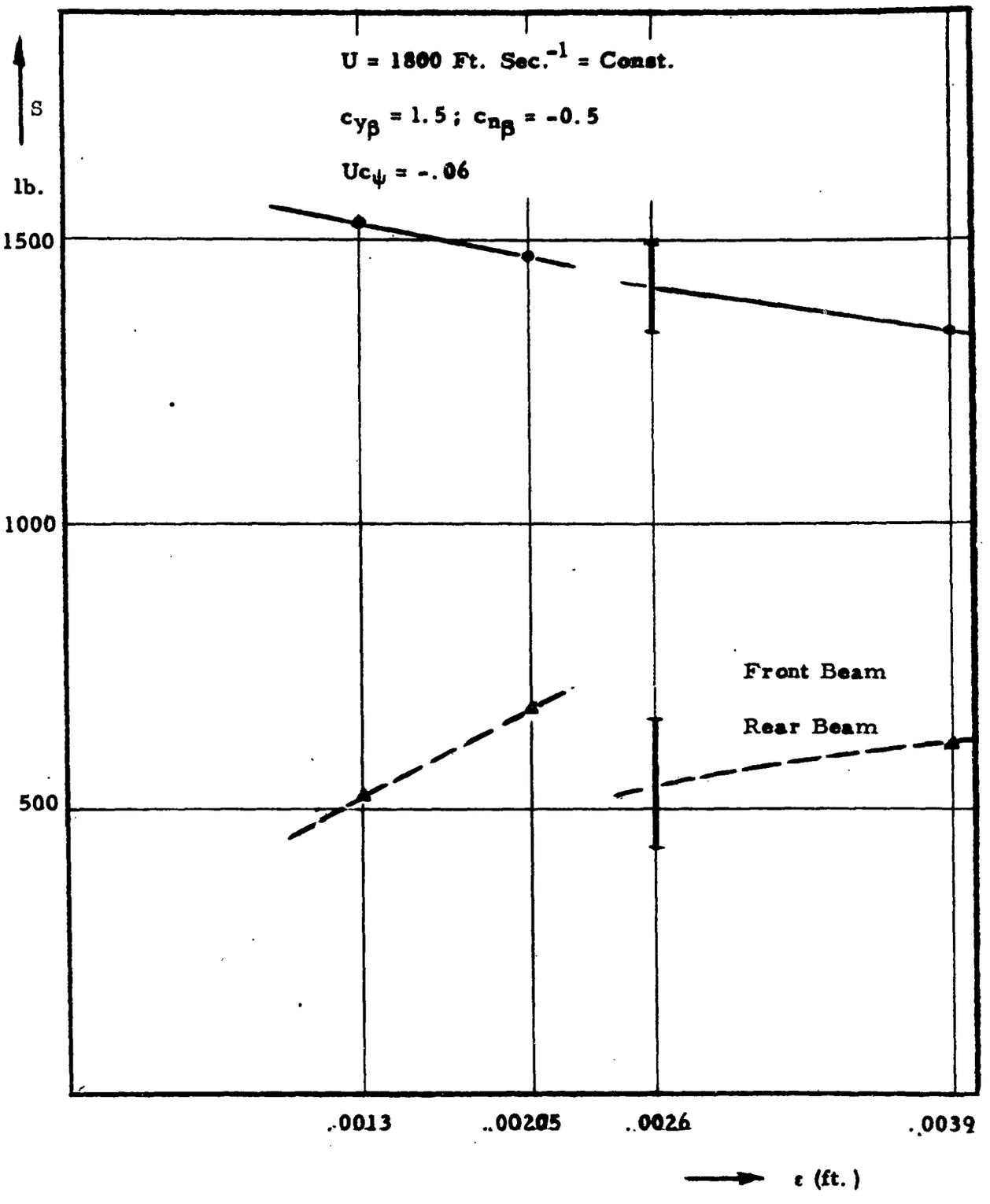

FIGURE 15. VARIATION OF THE SLIPPER FORCES S WITH SLIPPER PLAY ϵ

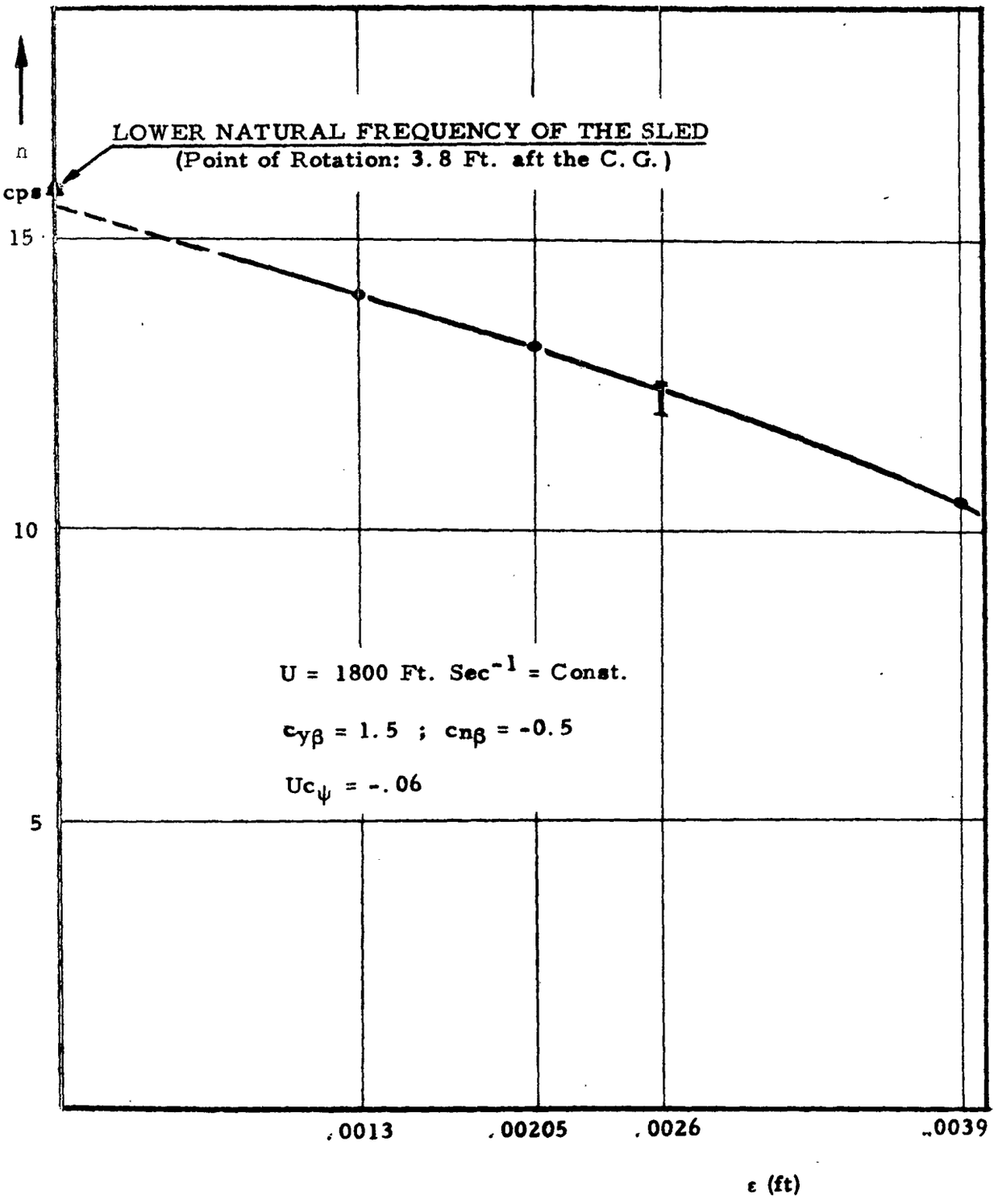

FIGURE 16. VARIATION OF THE FREQUENCY WITH SLIPPER PLAY ϵ

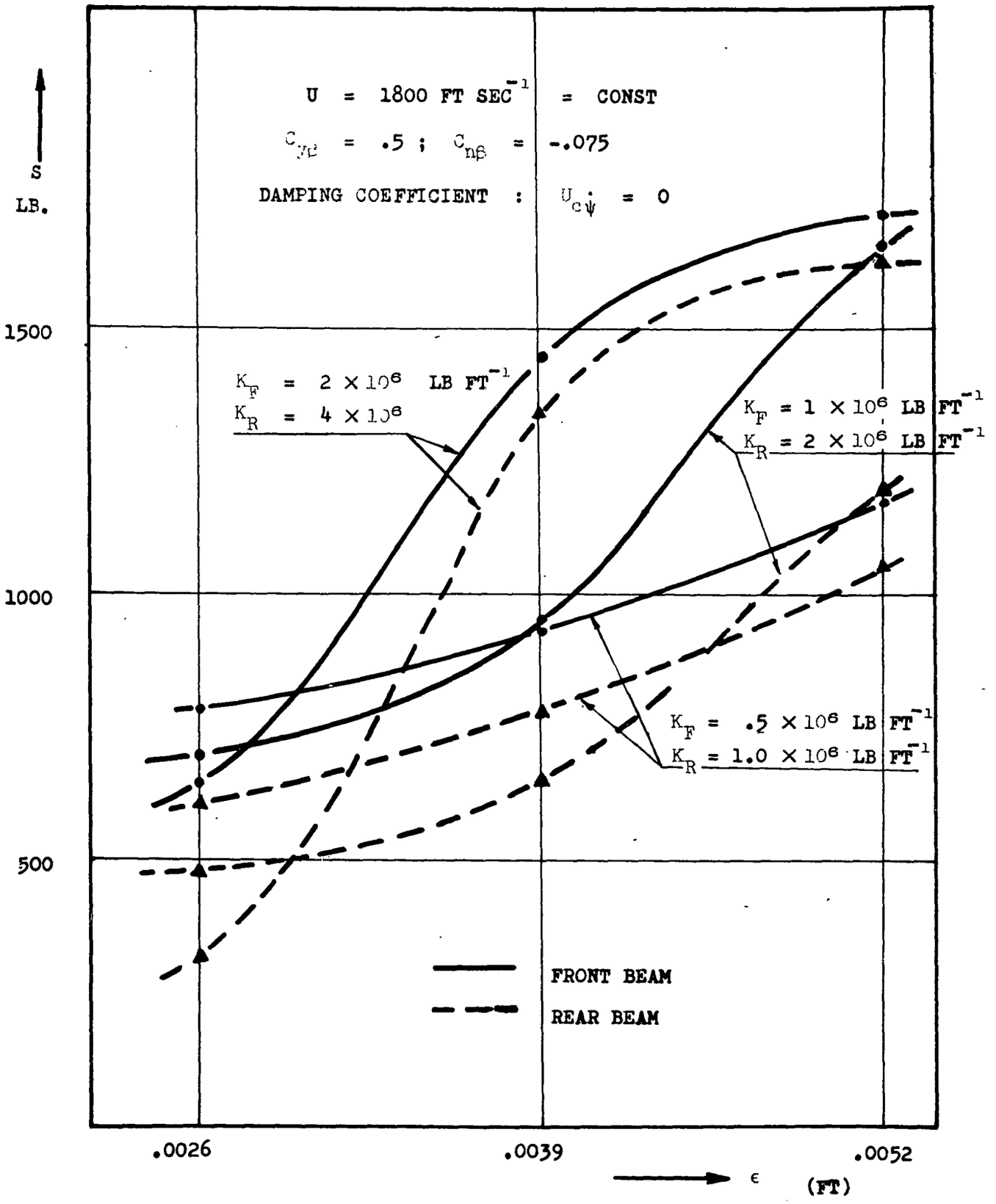

FIGURE 17. VARIATION OF THE SLIPPER FORCES S WITH SLIPPER PLAY ϵ
PARAMETER: SPRING CONSTANT K

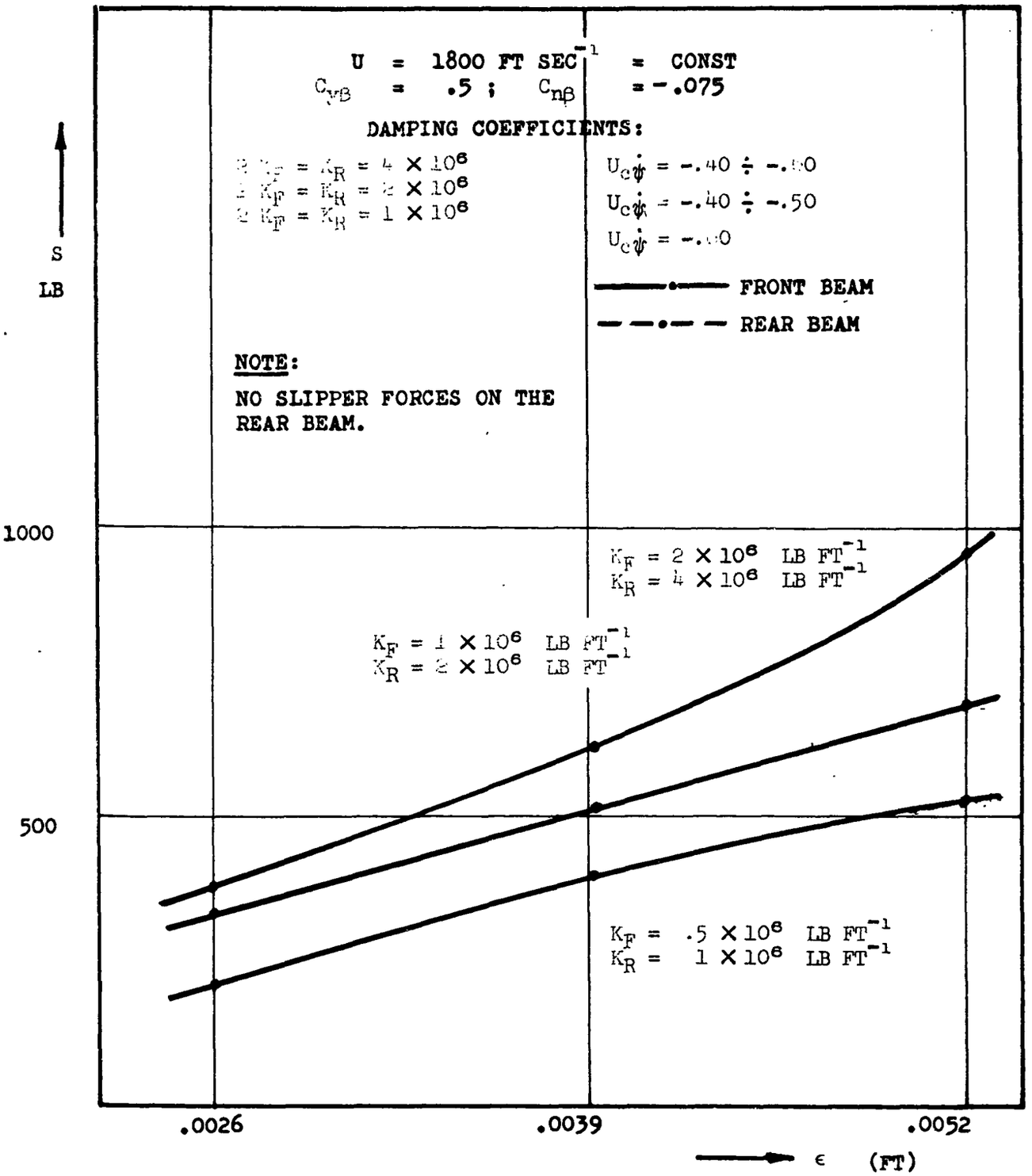

FIGURE 18. VARIATION OF THE SLIPPER FORCES S WITH SLIPPER PLAY ϵ
PARAMETER: SPRING CONSTANT K

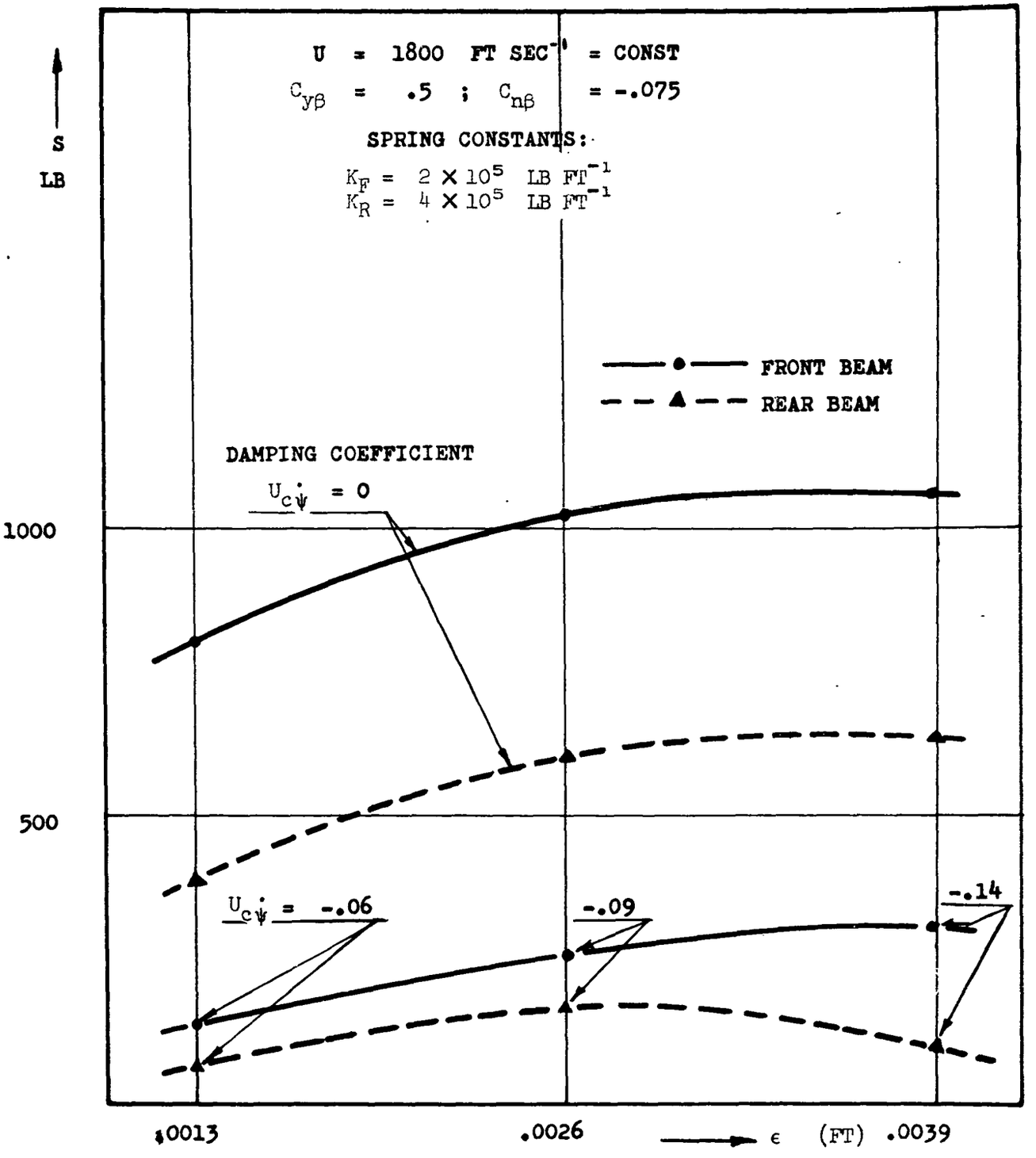

FIGURE 19. VARIATION OF THE SLIPPER FORCES S WITH SLIPPER PLAY ϵ
PARAMETER: DAMPING COEFFICIENT $U_c\dot{\psi}$

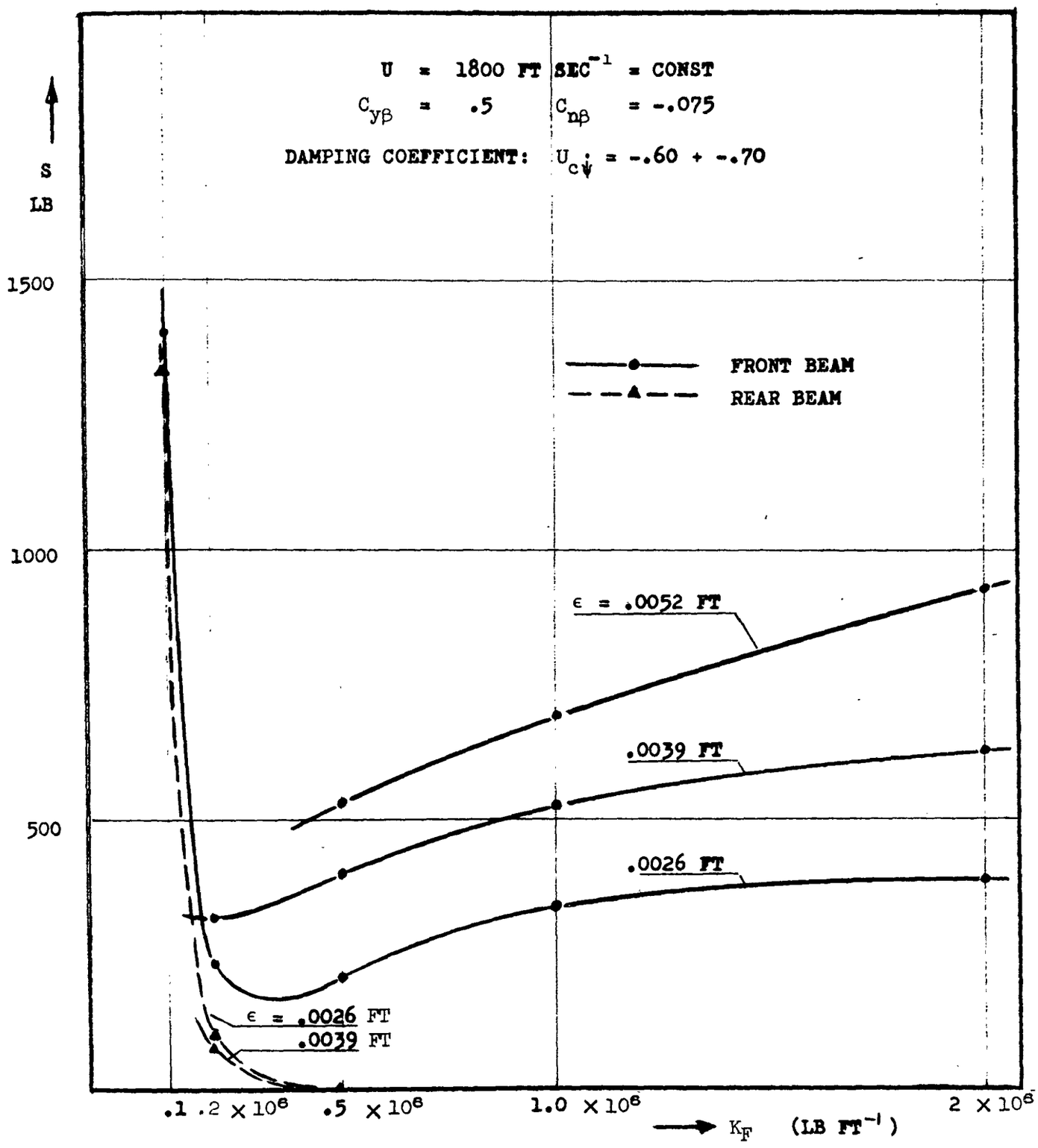

FIGURE 20. VARIATION OF THE SLIPPER FORCES S WITH THE SPRING CONSTANT K
PARAMETER: SLIPPER PLAY ϵ

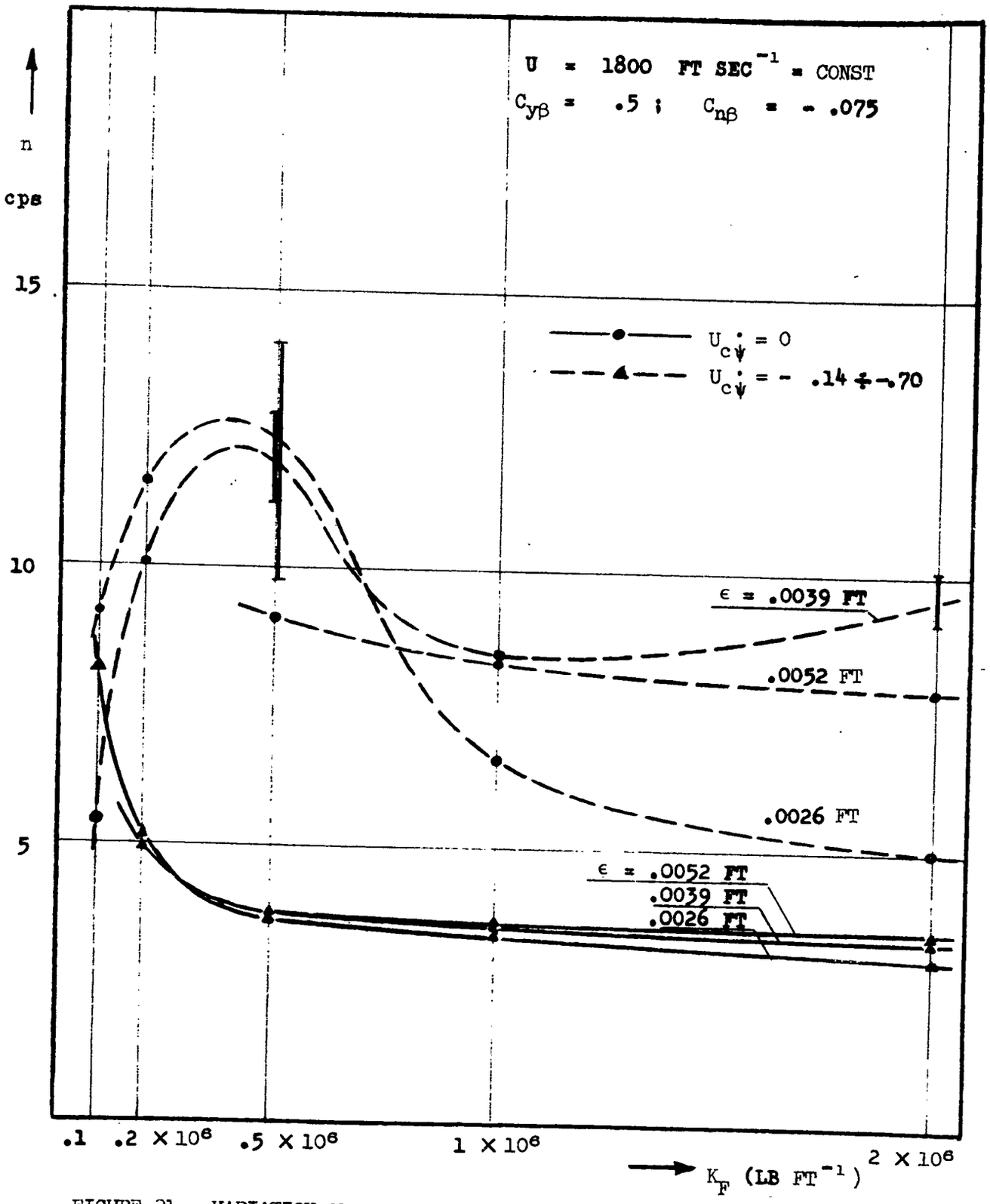

FIGURE 21. VARIATION OF THE DOMINANT FREQUENCY n WITH SPRING CONSTANT K
PARAMETER: SLIPPER PLAY ϵ

DISTRIBUTION

AFOSR (SRIL) 2
Wash 25, DC

NASA (Library) 2
1520 H Street NW
Wash 25, DC

Chief, R&D, Dept of the Army 1
ATTN: Scientific Information Branch
Wash 25, DC

AFSC (SCRS) 1
Andrews AFB
Wash 25, DC

Chairman 1
Canadian Joint Staff (DRB/DSIS)
2450 Massachusetts Avenue NW
Wash 25, DC

U. S. Naval Research Laboratory 1
ATTN: Library
Wash 25, DC

Institute of Technology (AU) 1
Library
MCLI-LIB, Bldg 125, Area B
Wright-Patterson AFB, Ohio

ASD (Technical Library) 1
Wright-Patterson AFB, Ohio

ARL (Technical Library) 2
Bldg 450
Wright-Patterson AFB, Ohio

High Speed Flight Station (NASA) 1
ATTN: Technical Library
Edwards AFB, Calif

AFFTC (FTOTL) 1
Edwards AFB, Calif

Ames Research Center (NASA) 1
ATTN: Technical Library
Moffett Field, Calif

RAND Corporation 2
1700 Main Street
Santa Monica, Calif

ASTIA (TIPCR) 20
Arlington Hall Station
Arlington 12, Va

Langley Research Center (NASA) 1
ATTN: Technical Library
Langley AFB, Va

Lewis Research Center (NASA) 1
ATTN: Technical Library
21000 Brookpark Road
Cleveland 35, Ohio

Commanding General 1
U. S. Army Ordnance Missile Command
ATTN: Technical Library
Redstone Arsenal, Ala

Institute of Aeronautical Sciences 1
2 East 64th Street
New York 21, NY

Applied Mechanics Reviews 2
Southwest Research Institute
8500 Culebra Road
San Antonio 6, Texas

AFCRL (CRRELA) 1
L. G. Hanscom Field, Mass

AEDC (AEOIM) 1
Arnold AF Stn., Tenn

Signal Corps Engineering Laboratory 1
(SIGFM/EL-RPO
Fort Monmouth, NJ

Linda Hall Library 1
ATTN: Documents Division
5109 Cherry Street
Kansas City 10, Mo

CIA (OCR Mail Room) 2
2430 E Street NW
Wash 25, DC

Detachment 1 1
Hq, Office of Aerospace Research
European Office, USAF
47 Cantersteen
Brussels, Belgium

Hq, USAF(AFCIN-3T) 1
Wash 25, DC

Hq, USAF (AFRDR-LS) 1
Wash 25, DC

Dept of the Navy 1
Bureau of Ordnance (Sp-401)
Wash 25, DC

AFMTC (Tech Library MU-135) 1
Patrick AFB, Fla

APGC (PGTRIL) 1
Eglin AFB, Fla

AFSWC (SWOI) 1
Kirtland AFB, NMex

AU (AUL-6008) 1
Maxwell AFB, Ala

RADC (RCOIL-2) 1
Griffiss AFB, NY

Dept of the Navy 1
Naval Research Laboratory
ATTN: Director, Code 5360
Wash 25, DC

Commanding Officer 1
Diamond Ordnance Fuse Laboratories
ATTN: Technical Reference Section
(ORDTL 06.33)
Wash 25, DC

USAFA (DLIB) 2
U. S. Air Force Academy, Colo

Analytic Services, Inc. 1
1101 North Royal Street
Alexandria, Va

School of Aeronautical and 1
Engineering Sciences
ATTN: Aero and ES Library
Purdue University
Lafayette, Ind

Space Technical Laboratories, Inc 1
ATTN: Information Services
Document Acquisition Group
P. O. Box 95001
Los Angeles 45, Calif

Commanding General 1
ATTN: ORDBS-OM-TL 312
White Sands Missile Range
NMex

Ordnance Mission 1
British Liaison Office
White Sands Missile Range
NMex

New Mexico State University of 1
Agriculture, Engineering, and Science
ATTN: Library
University Park, NMex

University of New Mexico 1
Government Publications Division
University of New Mexico Library
Albuquerque, NMex

Local

NLO	1
SRA	1
SRAT	3

Directorate of Research Analyses AF Office of Scientific Research Office of Aerospace Research Holloman AFB, New Mexico ON THE NONLINEAR YAW MOTION OF A ROCKET SLED. July 1962. 47 pp incl illus. AFOSR/DRA-62-13 unclassified report. Some results are presented of an analog computer study concerned with the motion of a rocket sled configuration within a prescribed velocity profile. The motion of the sled was sidewise restricted by slippers running on rails. (over)	UNCLASSIFIED I. Gerhard W. Braun II. Harald A. Melkus UNCLASSIFIED	Directorate of Research Analyses AF Office of Scientific Research Office of Aerospace Research Holloman AFB, New Mexico ON THE NONLINEAR YAW MOTION OF A ROCKET SLED. July 1962. 47 pp incl illus. AFOSR/DRA-62-13 unclassified report. Some results are presented of an analog computer study concerned with the motion of a rocket sled configuration within a prescribed velocity profile. The motion of the sled was sidewise restricted by slippers running on rails. (over)	UNCLASSIFIED I. Gerhard W. Braun II. Harald A. Melkus UNCLASSIFIED
Directorate of Research Analyses AF Office of Scientific Research Office of Aerospace Research Holloman AFB, New Mexico ON THE NONLINEAR YAW MOTION OF A ROCKET SLED. July 1962. 47 pp incl. illus. AFOSR/DRA-62-13 unclassified report. Some results are presented of an analog computer study concerned with the motion of a rocket sled configuration within a prescribed velocity profile. The motion of the sled was sidewise restricted by slippers running on rails. (over)	UNCLASSIFIED I. Gerhard W. Braun II. Harald A. Melkus UNCLASSIFIED	Directorate of Research Analyses AF Office of Scientific Research Office of Aerospace Research Holloman AFB, New Mexico ON THE NONLINEAR YAW MOTION OF A ROCKET SLED. July 1962. 47 pp incl. illus. AFOSR/DRA-62-13 unclassified report. Some results are presented of an analog computer study concerned with the motion of a rocket sled configuration within a prescribed velocity profile. The motion of the sled was sidewise restricted by slippers running on rails. (over)	UNCLASSIFIED I. Gerhard W. Braun II. Harald A. Melkus UNCLASSIFIED

The dynamic properties of the sled were studied under idealized conditions; it was assumed that the moving body has only two degrees of freedom: namely, lateral displacement and yaw. The body's weathercock stability was varied from negative to positive values as it was assumed that this aerodynamic property influences the mode of motion. The effects of damping and that of play between slipper and rail were studied to obtain indications as to how these parameters affect the motion.	UNCLASSIFIED UNCLASSIFIED	The dynamic properties of the sled were studied under idealized conditions; it was assumed that the moving body has only two degrees of freedom: namely, lateral displacement and yaw. The body's weathercock stability was varied from negative to positive values as it was assumed that this aerodynamic property influences the mode of motion. The effects of damping and that of play between slipper and rail were studied to obtain indications as to how these parameters affect the motion.	UNCLASSIFIED UNCLASSIFIED
The dynamic properties of the sled were studied under idealized conditions; it was assumed that the moving body has only two degrees of freedom: namely, lateral displacement and yaw. The body's weathercock stability was varied from negative to positive values as it was assumed that this aerodynamic property influences the mode of motion. The effects of damping and that of play between slipper and rail were studied to obtain indications as to how these parameters affect the motion.	UNCLASSIFIED UNCLASSIFIED	The dynamic properties of the sled were studied under idealized conditions; it was assumed that the moving body has only two degrees of freedom: namely, lateral displacement and yaw. The body's weathercock stability was varied from negative to positive values as it was assumed that this aerodynamic property influences the mode of motion. The effects of damping and that of play between slipper and rail were studied to obtain indications as to how these parameters affect the motion.	UNCLASSIFIED UNCLASSIFIED

Directorate of Research Analyses AF Office of Scientific Research Office of Aerospace Research Holloman AFB, New Mexico ON THE NONLINEAR YAW MOTION OF A ROCKET SLED. July 1962. 47 pp incl illus. AFOSR/DRA-62-13 unclassified report. Some results are presented of an analog computer study concerned with the motion of a rocket sled configuration within a prescribed velocity profile. The motion of the sled was sidewise restricted by slippers running on rails. (over)	UNCLASSIFIED I. Gerhard W. Braun II. Harald A. Melkus UNCLASSIFIED	Directorate of Research Analyses AF Office of Scientific Research Office of Aerospace Research Holloman AFB, New Mexico ON THE NONLINEAR YAW MOTION OF A ROCKET SLED. July 1962. 47 pp incl illus. AFOSR/DRA-62-13 unclassified report. Some results are presented of an analog computer study concerned with the motion of a rocket sled configuration within a prescribed velocity profile. The motion of the sled was sidewise restricted by slippers running on rails. (over)	UNCLASSIFIED I. Gerhard W. Braun II. Harald A. Melkus UNCLASSIFIED
Directorate of Research Analyses AF Office of Scientific Research Office of Aerospace Research Holloman AFB, New Mexico ON THE NONLINEAR YAW MOTION OF A ROCKET SLED. July 1962. 47 pp incl. illus. AFOSR/DRA-62-13 unclassified report. Some results are presented of an analog computer study concerned with the motion of a rocket sled configuration within a prescribed velocity profile. The motion of the sled was sidewise restricted by slippers running on rails. (over)	UNCLASSIFIED I. Gerhard W. Braun II. Harald A. Melkus UNCLASSIFIED	Directorate of Research Analyses AF Office of Scientific Research Office of Aerospace Research Holloman AFB, New Mexico ON THE NONLINEAR YAW MOTION OF A ROCKET SLED. July 1962. 47 pp incl. illus. AFOSR/DRA-62-13 unclassified report. Some results are presented of an analog computer study concerned with the motion of a rocket sled configuration within a prescribed velocity profile. The motion of the sled was sidewise restricted by slippers running on rails. (over)	UNCLASSIFIED I. Gerhard W. Braun II. Harald A. Melkus UNCLASSIFIED

The dynamic properties of the sled were studied under idealized conditions; it was assumed that the moving body has only two degrees of freedom: namely, lateral displacement and yaw. The body's weathercock stability was varied from negative to positive values as it was assumed that this aerodynamic property influences the mode of motion. The effects of damping and that of play between slipper and rail were studied to obtain indications as to how these parameters affect the motion.	UNCLASSIFIED UNCLASSIFIED	The dynamic properties of the sled were studied under idealized conditions; it was assumed that the moving body has only two degrees of freedom: namely, lateral displacement and yaw. The body's weathercock stability was varied from negative to positive values as it was assumed that this aerodynamic property influences the mode of motion. The effects of damping and that of play between slipper and rail were studied to obtain indications as to how these parameters affect the motion.	UNCLASSIFIED UNCLASSIFIED
The dynamic properties of the sled were studied under idealized conditions; it was assumed that the moving body has only two degrees of freedom: namely, lateral displacement and yaw. The body's weathercock stability was varied from negative to positive values as it was assumed that this aerodynamic property influences the mode of motion. The effects of damping and that of play between slipper and rail were studied to obtain indications as to how these parameters affect the motion.	UNCLASSIFIED UNCLASSIFIED	The dynamic properties of the sled were studied under idealized conditions; it was assumed that the moving body has only two degrees of freedom: namely, lateral displacement and yaw. The body's weathercock stability was varied from negative to positive values as it was assumed that this aerodynamic property influences the mode of motion. The effects of damping and that of play between slipper and rail were studied to obtain indications as to how these parameters affect the motion.	UNCLASSIFIED UNCLASSIFIED